

SUPPORTING INFORMATION

Conducting chiral nickel(II) bis(dithiolene) complexes: structural and electron transport modulation with the charge and the number of stereogenic centres

Alexandre Abhervé,^a Nabil Mroweh,^a Thomas Cauchy,^a Flavia Pop,^a HengBo Cui,^b Reizo Kato,^b Nicolas Vanthuyne,^c Pere Alemany,^d Enric Canadell*,^e and Narcis Avarvari*,^a

^a MOLTECH-Anjou, UMR 6200, CNRS, UNIV Angers, 2 bd Lavoisier, 49045 ANGERS Cedex, France. E-mail: narcis.avarvari@univ-angers.fr

^b Condensed Molecular Materials Laboratory, RIKEN, 2-1 Hirosawa, Wako, Saitama 351-0198, Japan

^c Aix Marseille Université, CNRS, Centrale Marseille, iSm2, Marseille, France

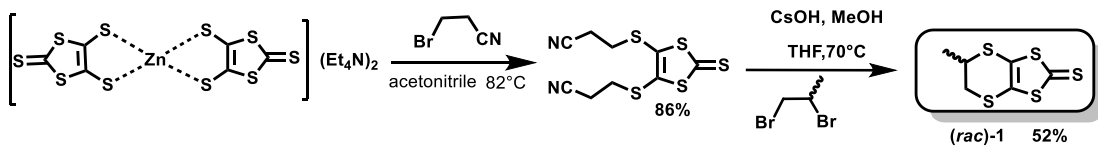
^d Departament de Ciència de Materials i Química Física i Institut de Química Teòrica i Computacional (IQT-CUB), Universitat de Barcelona, Martí i Franquès 1, 08028 Barcelona, Spain

^e Institut de Ciència de Materials de Barcelona, ICMAB-CSIC, Campus de la UAB, E-08193, Bellaterra, Spain. E-mail: canadell@icmab.es

Experimental section

General comments. Reactions of complexation were carried out under Argon atmosphere using the Schlenk technique. All compounds were obtained as single crystals and characterized by X-ray diffraction measurement. Elemental analysis were recorded using Flash 2000 Fisher Scientific Thermo Electron analyzer.

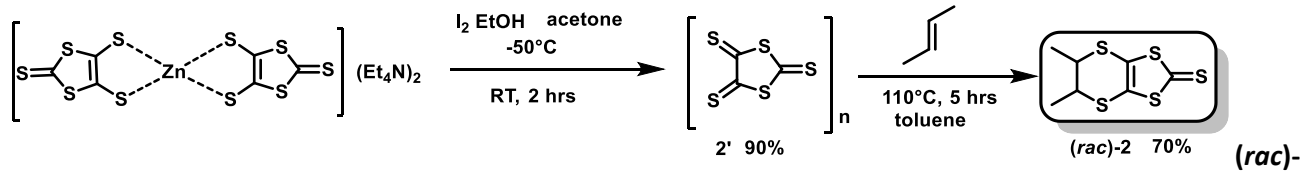
Synthesis of (*rac*)-1



(*rac*)-5,6-dihydro-5-methyl-1,3-dithiolo[4,5-*b*][1,4]dithiine-2-thione ((*rac*)-1): This compound was synthesized according to our procedure previously reported.

Reference: N. Mroweh, P. Auban-Senzier, N. Vanthuyne, E. Canadell and N. Avarvari, *J. Mater. Chem. C*, 2019, **7**, 12664–12673.

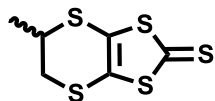
Synthesis of (*rac*)-2



5,6-Dihydro-5,6-dimethyl-1,3-dithiolo[4,5-*b*][1,4]dithiin-2-thione ((*rac*)-2): The trithione **2'** has been prepared according to the literature procedure: N.Svenstrup and J. Becher, *Synthesis*, 1995, 215–235. Then, for the preparation of (*rac*)-2, we have modified the procedure briefly described in: G. C. Papavassiliou, G. A. Mousdis and A. Papadima, *Z. Naturforsch. B*, 2000, **55**, 231–232. Trithione **2'** (2 g, 0.01 mol) was added into a closed vessel containing 140 mL of toluene. Gaseous *trans*-2-butene (0.02 mol) has been pumped into this vessel and the mixture was refluxed for two hours at 110 °C. The solvent was then evaporated using rotary evaporator, and the crude product purified by column chromatography using petroleum spirit/dichloromethane 8/2 as eluent to afford a yellowish solid (2 g, 70%). The spectral data for (*rac*)-2 thus obtained match those reported in the literature: F. Pop, P. Auban-Senzier, A. Frąckowiak, K. Ptaszyński, I. Olejniczak, J. D. Wallis, E. Canadell and N. Avarvari, *J. Am. Chem. Soc.*, 2013, **135**, 17176–17186.

Chiral HPLC

Analytical chiral HPLC separation for compound (*rac*)-1



- The sample is dissolved in dichloromethane, injected on the chiral column, and detected with an UV detector at 254 nm and a circular dichroism detector at 254 nm. The flow-rate is 1 mL/min.

Column	Mobile Phase	t ₁	k ₁	t ₂	k ₂	α	Rs
Chiraldak IF	Heptane / dichloromethane (80/20)	12.14 (-)	3.12	13.20 (+)	3.48	1.12	2.39

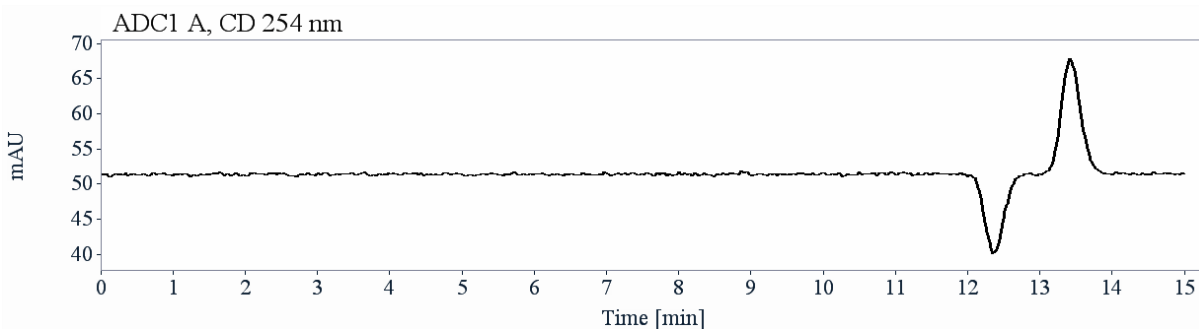
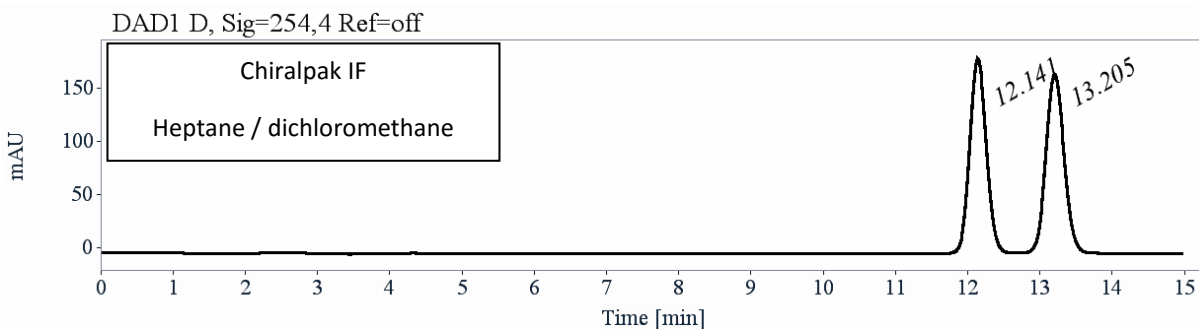


Fig. S1 Analytical chiral HPLC separation for compound (*rac*)-1.

RT [min]	Area	Area%	Capacity Factor	Enantioselectivity	Resolution (USP)
12.14	2945	49.94	3.12		
13.20	2952	50.06	3.48	1.12	2.39

Sum	5897	100.00		
-----	------	--------	--	--

Semi-preparative separation for compound (*rac*)-1:

- Sample preparation: About 250 mg of compound (*rac*)-1 are dissolved in 8 mL of dichloromethane.
- Chromatographic conditions: Chiralpak IF (250 x 10 mm), hexane / dichloromethane (80/20) as mobile phase, flow-rate = 5 mL/min, UV detection at 254 nm.
- Injections (stacked): 270 times 30 µL, every 5 minutes.
- First fraction: 95 mg of the first eluted ((-, CD 254nm)-enantiomer) with ee > 99 %
- Second fraction: 72 mg of the second eluted ((+, CD 254 nm)-enantiomer) with ee > 98%
- Chromatograms of the collected fractions:

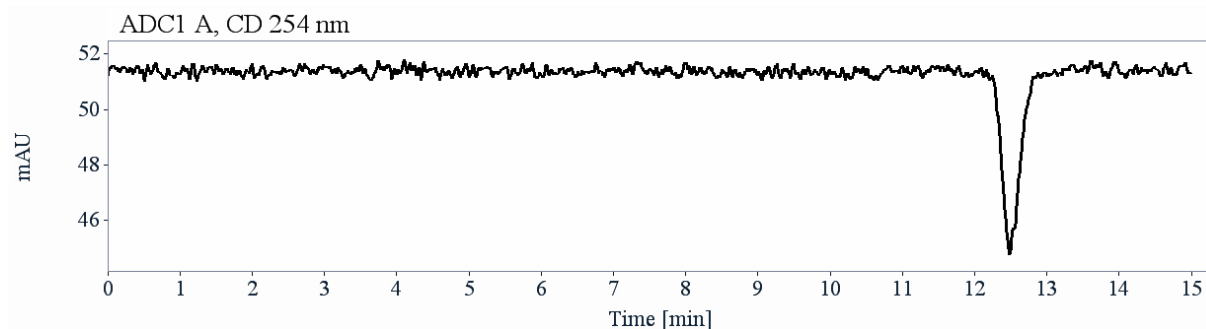
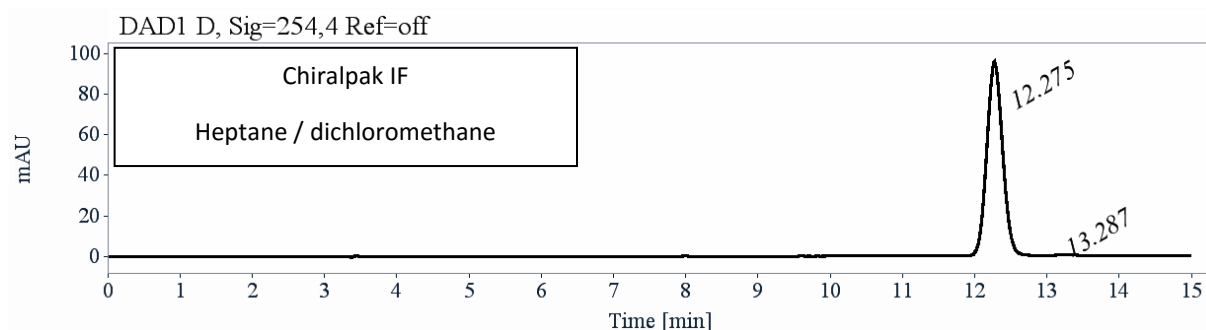


Fig. S2 Chiral HPLC separation for compound (*S*)-1.

RT [min]	Area	Area%
12.27	1464	99.51
13.29	7	0.49
Sum	1471	100.00

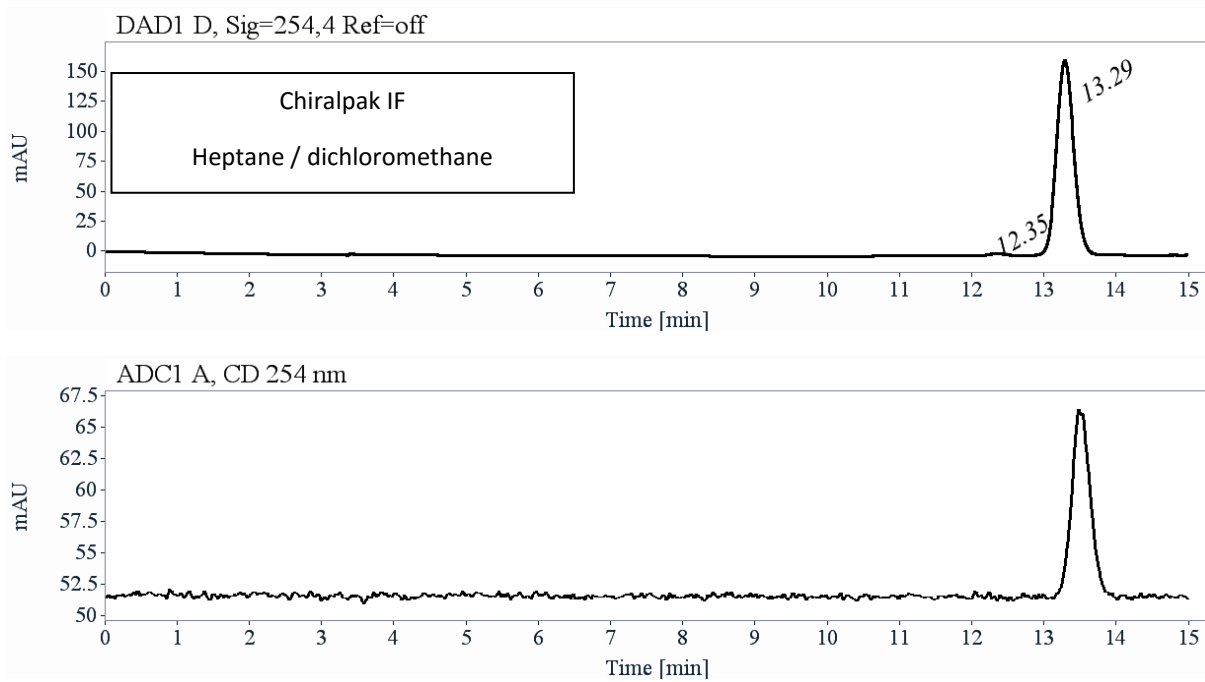


Fig. S3 Chiral HPLC separation for compound *(R)*-1.

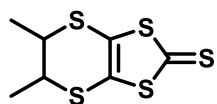
RT [min]	Area	Area%
12.35	25	0.92
13.29	2720	99.08
Sum	2746	100.00

Optical rotations

Optical rotations were measured on a Jasco P-2000 polarimeter with a sodium lamp (589 nm), a halogen lamp (578 nm and 546 nm), in a 10 cm cell, thermostated at 25°C with a Peltier controlled cell holder.

λ (nm)	<i>(S)</i> -1 first eluted on Chiraldak IF $[\alpha]_{\lambda}^{25}$ (CH_2Cl_2 , c = 0.085)	<i>(R)</i> -1 second eluted on Chiraldak IF $[\alpha]_{\lambda}^{25}$ (CH_2Cl_2 , c = 0.088)
589	- 48	+ 48
578	- 45	+ 45
546	- 18	+ 18

Analytical chiral HPLC separation for compound (*rac*)-2



- The sample is dissolved in dichloromethane, injected on the chiral column, and detected with an UV detector at 254 nm and a circular dichroism detector at 254 nm. The flow-rate is 1 mL/min.

Column	Mobile Phase	t ₁	k ₁	t ₂	k ₂	α	Rs
Chiraldak ID	Heptane / dichloromethane (90/10)	11.09 (-)	2.76	12.15 (+)	3.12	1.13	2.18

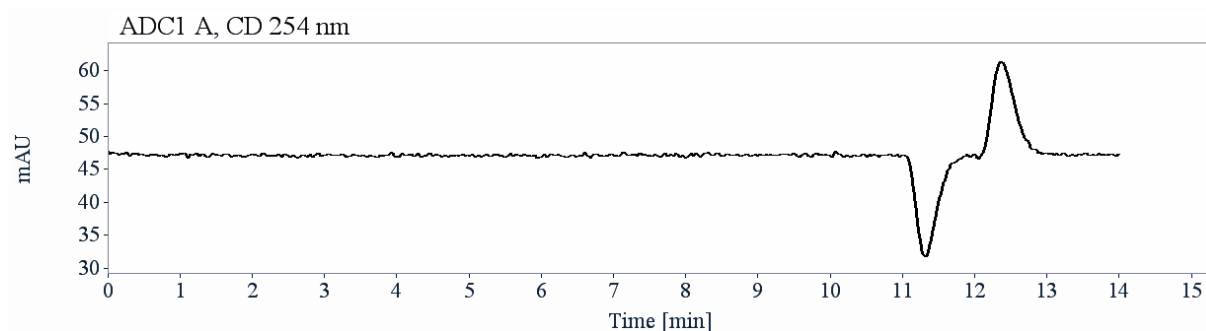
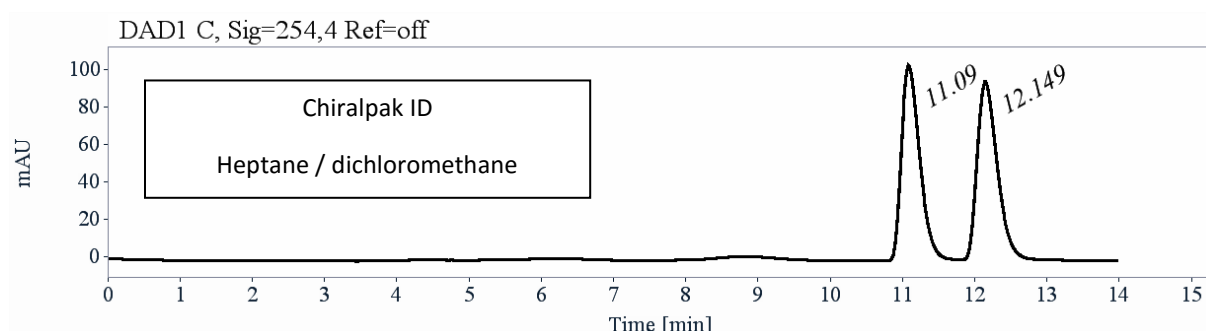


Fig. S4 Analytical chiral HPLC separation for compound (*rac*)-2.

RT [min]	Area	Area%	Capacity Factor	Enantioselectivity	Resolution (USP)
11.09	1847	49.89	2.76		
12.15	1856	50.11	3.12	1.13	2.18

Sum	3703	100.00			
-----	------	--------	--	--	--

Semi-preparative separation for compound (*rac*)-2:

- Sample preparation: About 312 mg of compound (*rac*)-2 are dissolved in 10 mL of dichloromethane.
- Chromatographic conditions: Chiraldak ID (250 x 10 mm), hexane / dichloromethane (90/10) as mobile phase, flow-rate = 5 mL/min, UV detection at 254 nm.
- Injections (stacked): 200 times 50 µL, every 4.8 minutes.
- First fraction: 134 mg of the first eluted with ee > 96 %
- Second fraction: 135 mg of the second eluted with ee > 94.5%
- Intermediate: 35 mg
- Chromatograms of the collected fractions:

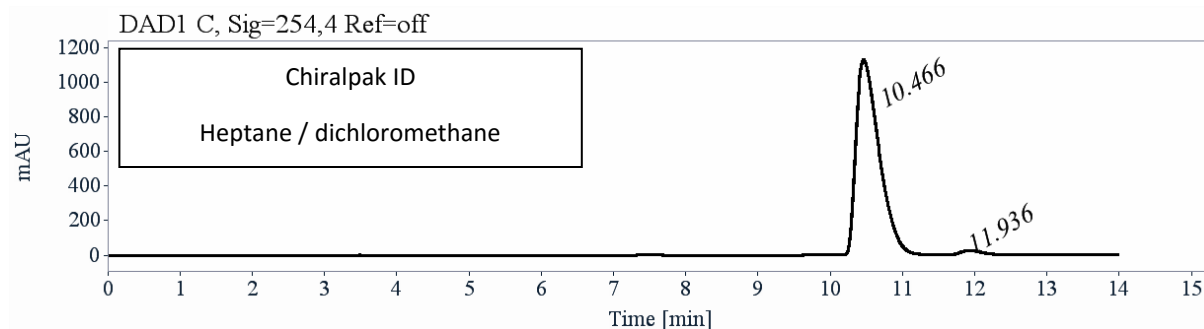


Fig. S5 Chiral HPLC separation for compound (*S,S*)-2.

RT [min]	Area	Area%
10.47	25327	98.08
11.94	497	1.92
Sum	25824	100.00

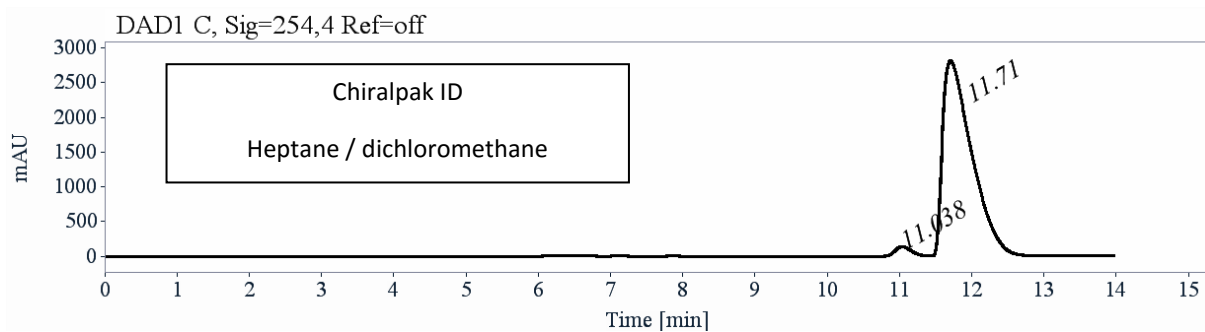


Fig. S6 Chiral HPLC separation for compound *(R,R)-2*.

RT [min]	Area	Area%
11.04	2149	2.66
11.71	78616	97.34
Sum	80766	100.00

Optical rotations

Optical rotations were measured on a Jasco P-2000 polarimeter with a sodium lamp (589 nm), a halogen lamp (578 nm and 546 nm), in a 10 cm cell, thermostated at 25°C with a Peltier controlled cell holder.

λ (nm)	<i>(S,S)-2</i> first eluted on Chiraldak ID $[\alpha]_{\lambda}^{25}$ (CH_2Cl_2 , c = 0.07)	<i>(R,R)-2</i> second eluted on Chiraldak ID $[\alpha]_{\lambda}^{25}$ (CH_2Cl_2 , c = 0.07)
589	- 371	+ 365
578	- 400	+ 393
546	- 560	+ 553

Electronic Circular Dichroism (ECD) and UV-Visible spectroscopy

ECD and UV spectra were measured on a JASCO J-815 spectrometer equipped with a JASCO Peltier cell holder PTC-423 to maintain the temperature at $25.0 \pm 0.2^\circ\text{C}$. A CD quartz cell of 1 mm of optical pathlength was used. The CD spectrometer was purged with nitrogen before recording each spectrum, which was baseline subtracted. The baseline was always measured for the same solvent and in the same cell as the samples. The spectra are presented without smoothing and further data processing.

Compound 1

(*S*)-1, first eluted on Chiralpak IF: green solid line, concentration = 1.25 mmol.L^{-1} in acetonitrile.

(*R*)-1, second eluted on Chiralpak IF: red dotted line, concentration = 1.25 mmol.L^{-1} in acetonitrile.

Acquisition parameters: 0.1 nm as intervals, scanning speed 50 nm/min, band width 2 nm, and 3 accumulations per sample.

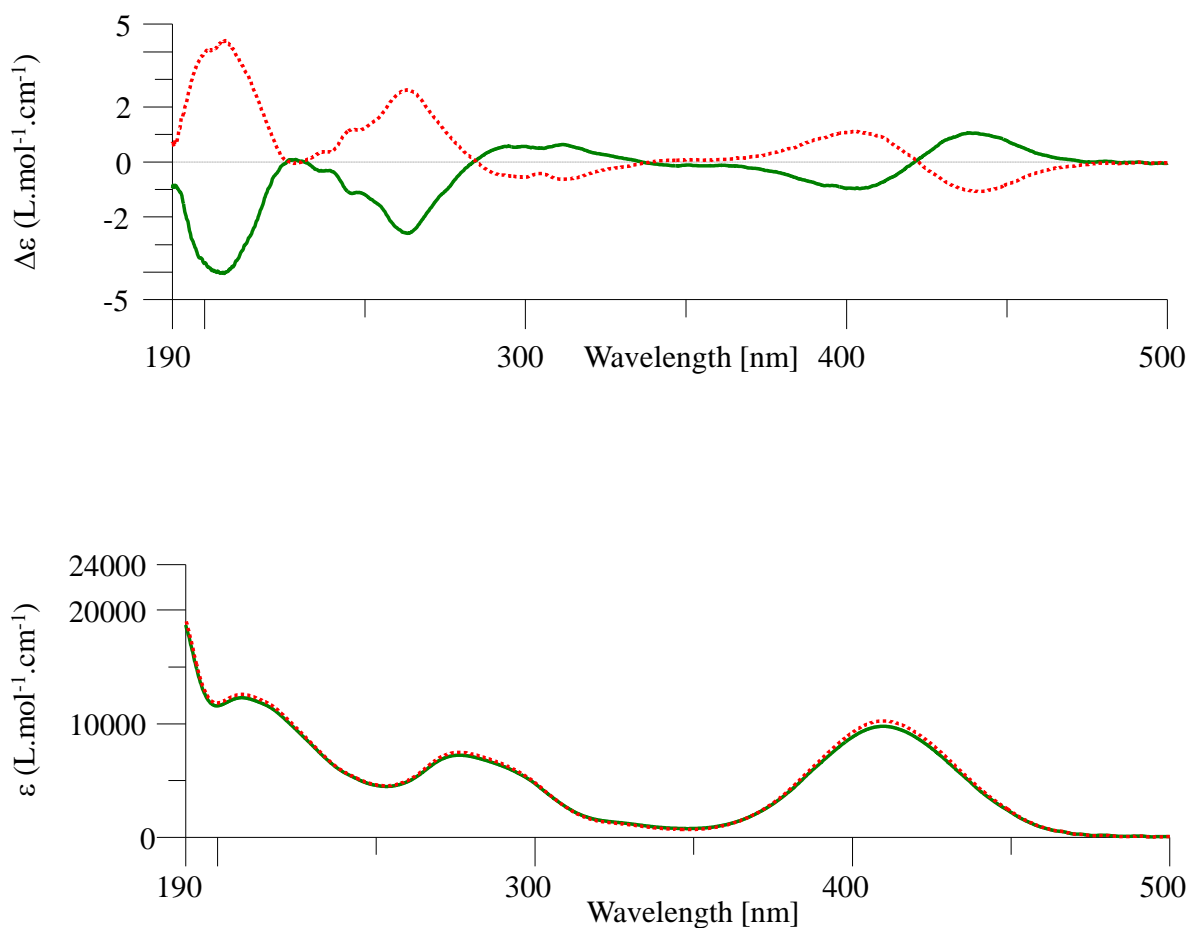


Fig. S7 CD (top) and UV-Vis (bottom) spectra of (*S*)-1 (green line) and (*R*)-1 (red dotted line).

Compound 2

(*S,S*)-2, first eluted on Chiralpak ID: green solid line, concentration = 0.815 mmol.L⁻¹ in acetonitrile.

(*R,R*)-2, second eluted on Chiralpak ID: red dotted line, concentration = 0.816 mmol.L⁻¹ in acetonitrile.

Acquisition parameters: 0.1 nm as intervals, scanning speed 50 nm/min, band width 2 nm, and 3 accumulations per sample.

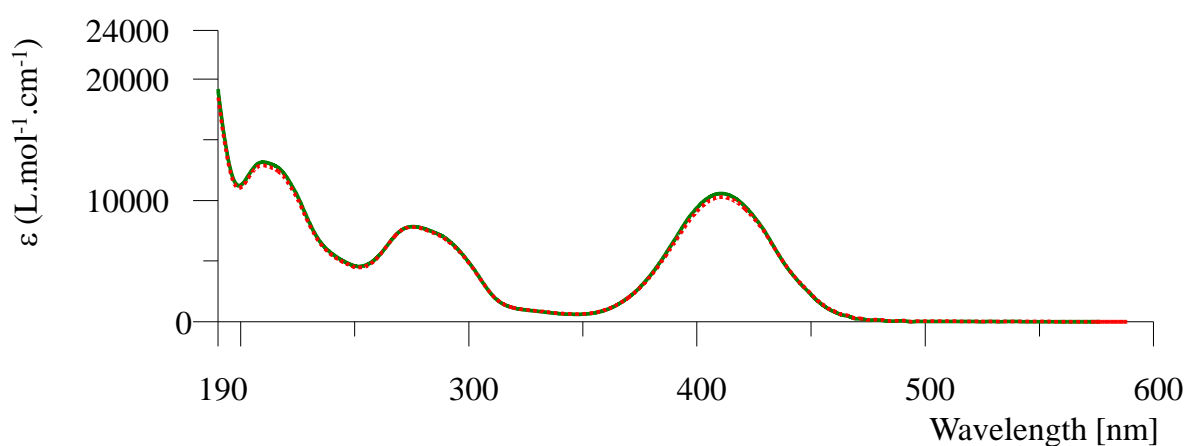
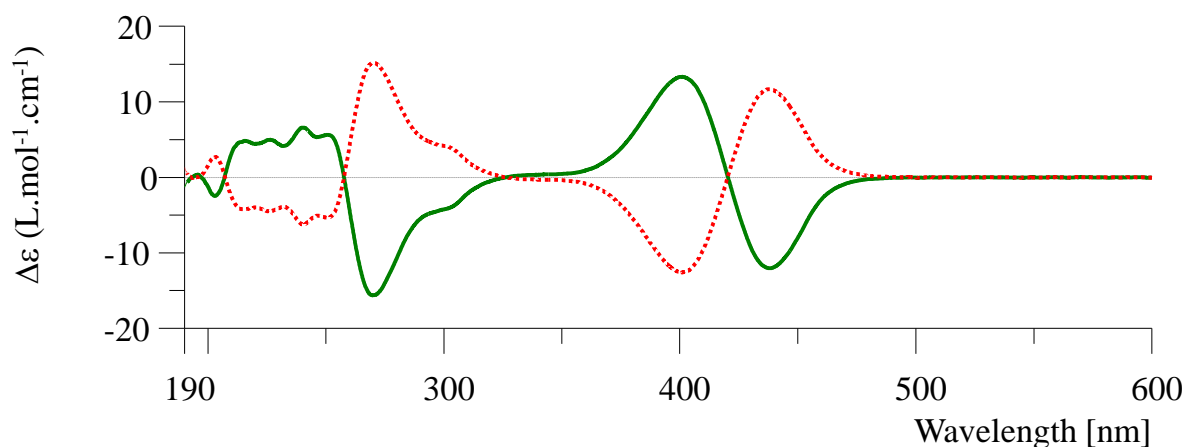


Fig. S8 CD (top) and UV-Vis (bottom) spectra of (*S,S*)-2 (green line) and (*R,R*)-2 (red dotted line).

DFT and TD-DFT calculations

Compound (*R*)-1, axial conformation

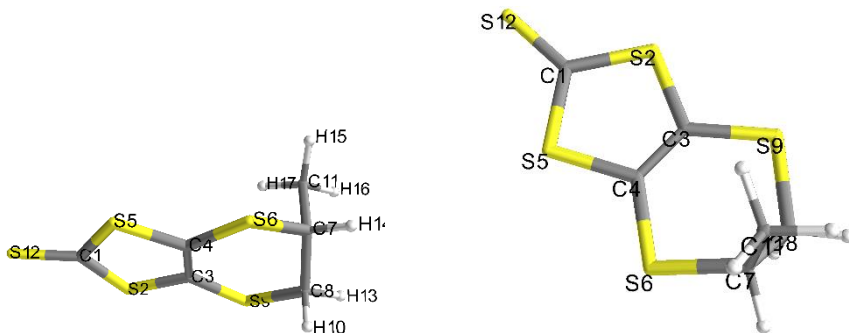


Fig. S9 Two views of the optimized geometry of axial (*R*)-1 together with the atom numbering scheme.

Total molecular energy	-2222.32542 hartrees
HOMO number	61
LUMO+1 energies	-0.86 eV
LUMO energies	-1.92 eV
HOMO energies	-5.99 eV
HOMO-1 energies	-6.60 eV

Geometry optimization specific results	
Converged nuclear repulsion energy	1133.85712 Hartrees
Frequency and Thermochemistry specific results	
Number of negative frequencies	0
Sum of electronic and zero-point energy	-2222.21604 Hartrees
Sum of electronic and thermal energies at 298.15 K	-2222.20453 Hartrees
Enthalpy at 298.15 K	-2222.20358 Hartrees
Gibbs free energy at 298.15 K	-2222.25506 Hartrees
Entropy at 298.15 K	0.00017 Hartrees

E.S.	Symmetry	Calculated mono-electronic excitations							qCT Excitation description in %
		nm	cm ⁻¹	f	R	Lambda	dCT		
1	Singlet-A	410	24357	0.001	28.812	0.47	114.73	0.75	60->62 (95) 61->62 (4)
2	Singlet-A	360	27722	0.118	-37.983	0.60	295.20	0.61	59->62 (2) 60->62 (3) 61->62 (92)
3	Singlet-A	324	30829	0.001	-2.759	0.49	47.82	0.74	61->63 (96) 61->64 (2)
4	Singlet-A	287	34796	0.032	34.485	0.64	185.28	0.50	58->62 (6) 61->63 (2) 61->64 (85) 61->66 (2)
5	Singlet-A	272	36669	0.001	0.405	0.36	265.62	0.78	58->62 (6) 60->63 (90)
6	Singlet-A	271	36836	0.001	2.048	0.47	237.26	0.72	59->65 (2) 61->65 (94)
7	Singlet-A	261	38225	0.104	10.730	0.60	276.27	0.54	59->62 (91) 60->69 (3)
8	Singlet-A	254	39273	0.011	11.562	0.38	281.40	0.56	58->62 (70) 60->63 (4) 60->64 (6) 61->66 (12)
9	Singlet-A	249	40111	0.003	13.038	0.23	446.32	0.84	58->62 (2) 60->63 (2) 60->64 (90)
10	Singlet-A	237	42095	0.037	2.387	0.50	168.68	0.52	58->62 (9) 59->63 (18) 59->64 (11) 61->64 (5) 61->66 (42) 61->67 (6)
11	Singlet-A	236	42322	0.008	-39.742	0.42	2.36	0.68	58->62 (2) 58->65 (2) 59->63 (75) 61->66 (12)
12	Singlet-A	228	43828	0.000	1.029	0.45	179.35	0.72	57->63 (2) 58->63 (86) 59->65 (5)

13	Singlet-A	224	44516	0.007	1.014	0.48	363.01	0.66 61->66 (8) 61->67 (70) 61->68 (15)
14	Singlet-A	223	44825	0.027	22.367	0.49	212.75	0.62 58->64 (3) 59->64 (78) 61->66 (11)
15	Singlet-A	222	45004	0.042	-4.014	0.24	515.10	0.86 60->65 (94)

Atomic charges population analysis. Selection of the most charged atoms based on Hirshfeld analysis

Atom and N°	Hirshfeld charge	CM5 charge	Mulliken charge
C 11	-0.258	-0.112	-0.319
S 12	-0.182	-0.199	-0.136
C 8	-0.169	-0.058	-0.329
S 5	+0.126	+0.099	+0.225

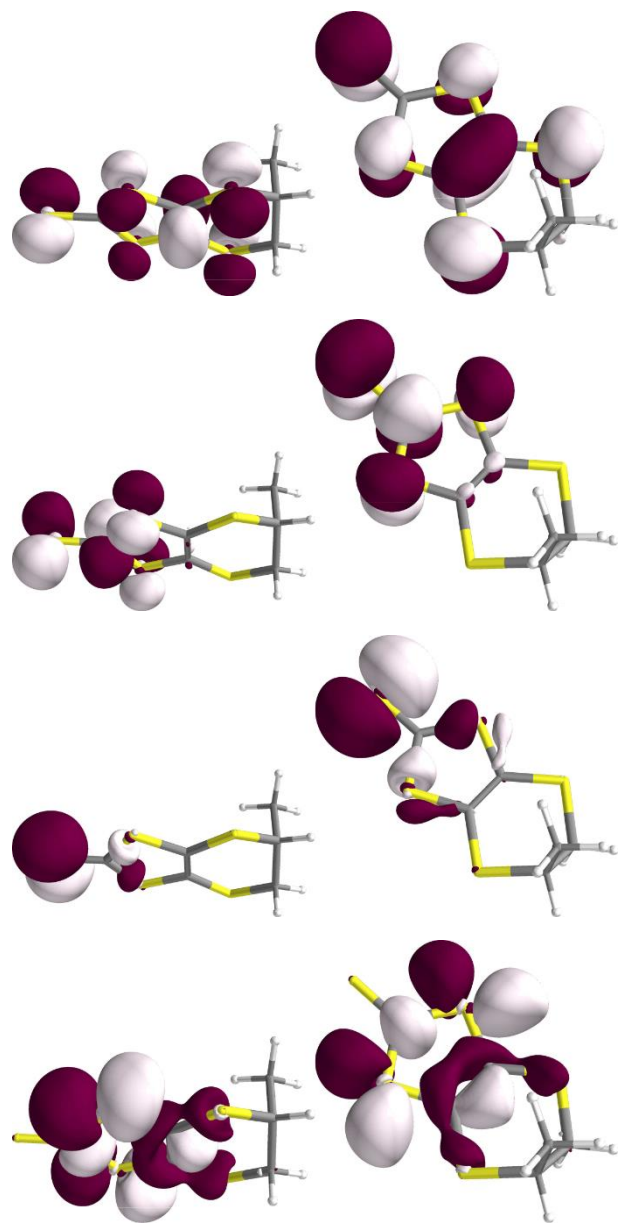


Fig. S10 HOMO, LUMO, HOMO-1 and LUMO+1 (from top to bottom, two views each) of axial (*R*)-1.

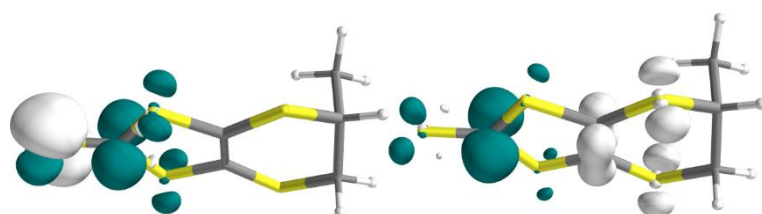


Fig. S11 Representation of the Electron Density Difference (S1-S0 left) and (S2-S0 right) of axial (*R*)-1. The excited electron and hole regions are indicated by respectively blue and white surfaces.

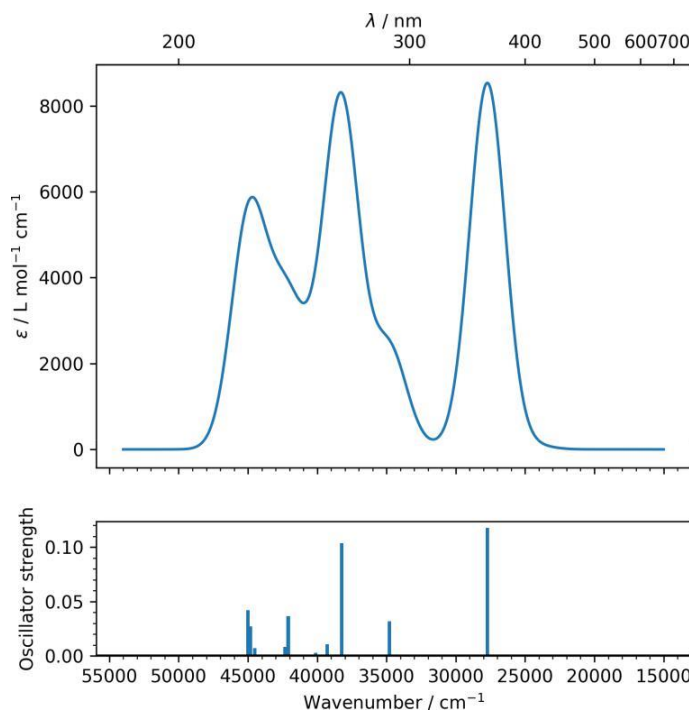


Fig. S12 Calculated UV-vis absorption spectrum of axial (R)-1 with a gaussian broadening (FWHM = 3000 cm^{-1}).

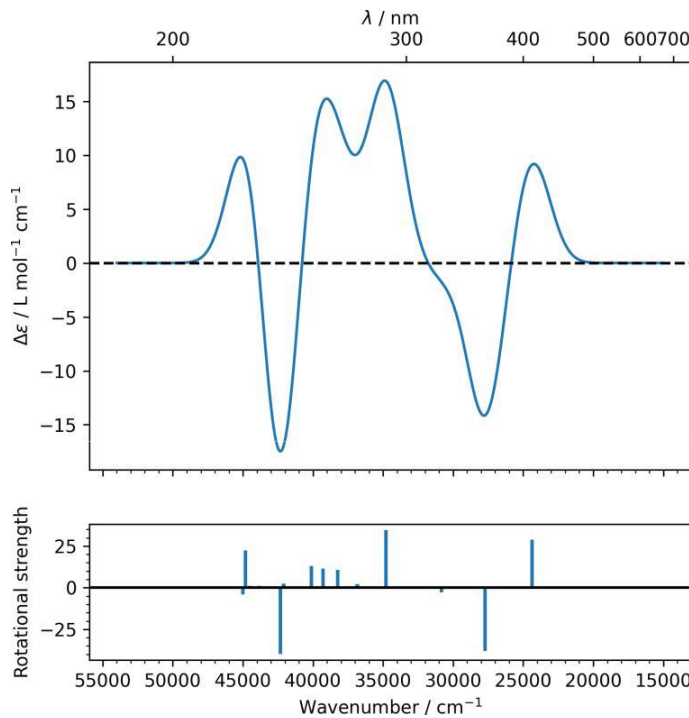


Fig. S13 Calculated CD spectrum of axial (R)-1 with a gaussian broadening (FWHM = 3000 cm^{-1}).

Compound (S)-1, axial conformation

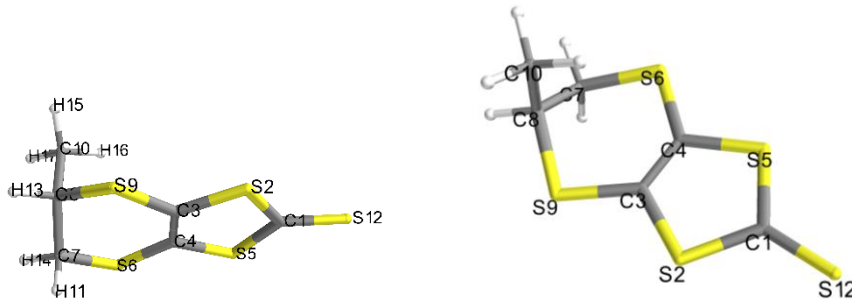


Fig. S14 Two views of the optimized geometry of axial (S)-1 together with the atom numbering scheme.

Total molecular energy -2222.32542 hartrees

HOMO number	61
LUMO+1 energies	-0.86 eV
LUMO energies	-1.92 eV
HOMO energies	-5.99 eV
HOMO-1 energies	-6.60 eV

Geometry optimization specific results
Converged nuclear repulsion energy 1133.84361 Hartrees

Frequency and Thermochemistry specific results
Number of negative frequencies 0
Sum of electronic and zero-point energy -2222.21604 Hartrees
Sum of electronic and thermal energies at 298.15 K -2222.20453 Hartrees
Enthalpy at 298.15 K -2222.20358 Hartrees
Gibbs free energy at 298.15 K -2222.25507 Hartrees
Entropy at 298.15 K 0.00017 Hartrees

E.S.	Symmetry	Calculated mono-electronic excitations						
		nm	cm-1	f	R	Lambda dCT	qCT	Excitation description in %
1	Singlet-A	410	24357	0.001	-28.811	0.47	114.74	0.75 60->62 (95) 61->62 (4)
2	Singlet-A	360	27722	0.118	37.985	0.60	295.21	0.61 59->62 (2) 60->62 (3) 61->62 (92)
3	Singlet-A	324	30830	0.001	2.748	0.49	47.95	0.74 61->63 (96) 61->64 (2)
4	Singlet-A	287	34797	0.032	-34.477	0.64	185.39	0.50 58->62 (6) 61->63 (2) 61->64 (85) 61->66 (2)
5	Singlet-A	272	36669	0.001	-0.413	0.36	265.52	0.78 58->62 (6) 60->63 (90)
6	Singlet-A	271	36839	0.001	-2.046	0.47	237.16	0.72 59->65 (2) 61->65 (94)
7	Singlet-A	261	38225	0.104	-10.729	0.60	276.25	0.54 59->62 (91) 60->69 (3)
8	Singlet-A	254	39274	0.011	-11.579	0.38	281.63	0.56 58->62 (70) 60->63 (4) 60->64 (6) 61->66 (12)
9	Singlet-A	249	40113	0.003	-13.039	0.23	446.36	0.84 58->62 (2) 60->63 (2) 60->64 (90)
10	Singlet-A	237	42098	0.036	-2.670	0.50	167.87	0.52 58->62 (9) 59->63 (19) 59->64 (11) 61->64 (5) 61->66 (42) 61->67 (6)
11	Singlet-A	236	42324	0.008	40.039	0.42	2.42	0.68 58->62 (2) 58->65 (2) 59->63 (75) 61->66 (12)
12	Singlet-A	228	43829	0.000	-1.027	0.45	179.51	0.72 57->63 (2) 58->63 (86) 59->65 (5)

13	Singlet-A	224	44513	0.007	-0.934	0.48	363.05	0.66 61->66 (8) 61->67 (70) 61->68 (15)
14	Singlet-A	223	44828	0.027	-22.437	0.49	212.95	0.62 58->64 (3) 59->64 (78) 61->66 (11)
15	Singlet-A	222	45007	0.042	3.989	0.24	515.04	0.86 60->65 (94)

Atomic charges population analysis. Selection of the most charged atoms based on Hirshfeld analysis

Atom and N°	Hirshfeld charge	CM5 charge	Mulliken charge
C 10	-0.258	-0.112	-0.319
S 12	-0.182	-0.199	-0.136
C 7	-0.149	-0.058	-0.329
H 13	+0.120	+0.060	+0.189
S 5	+0.126	+0.099	+0.221

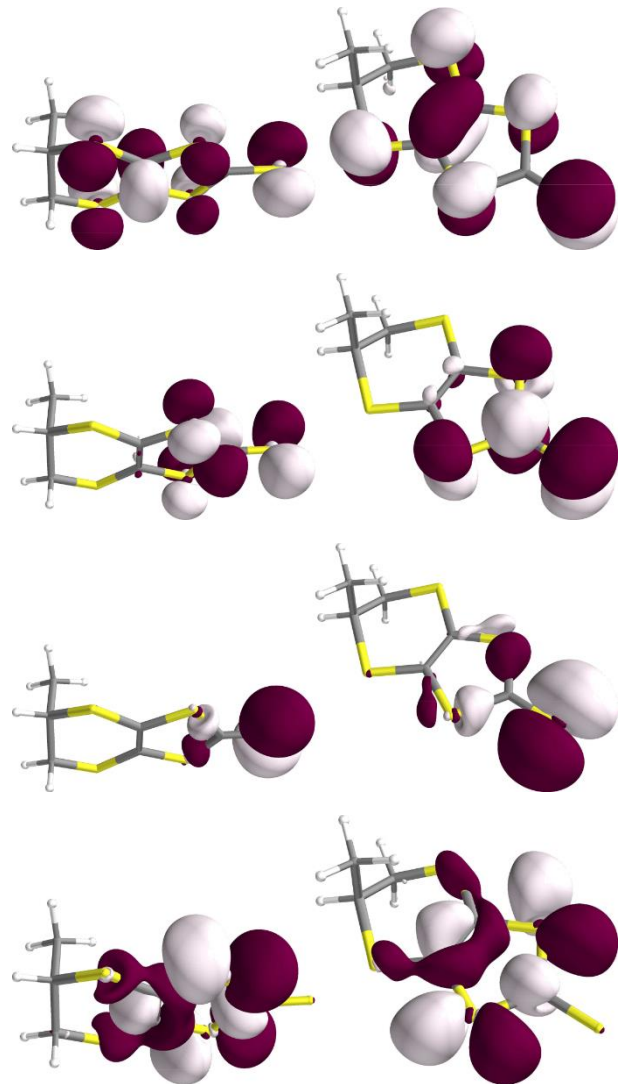


Fig. S15 HOMO, LUMO, HOMO-1 and LUMO+1 (from top to bottom, two views each) of axial (S)-1.

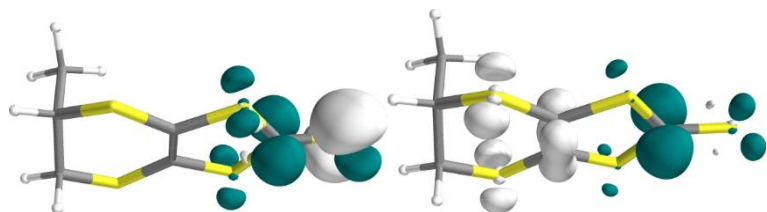


Fig. S16 Representation of the Electron Density Difference (S_1-S_0 left) and (S_2-S_0 right) of axial (S)-1. The excited electron and hole regions are indicated by respectively blue and white surfaces.

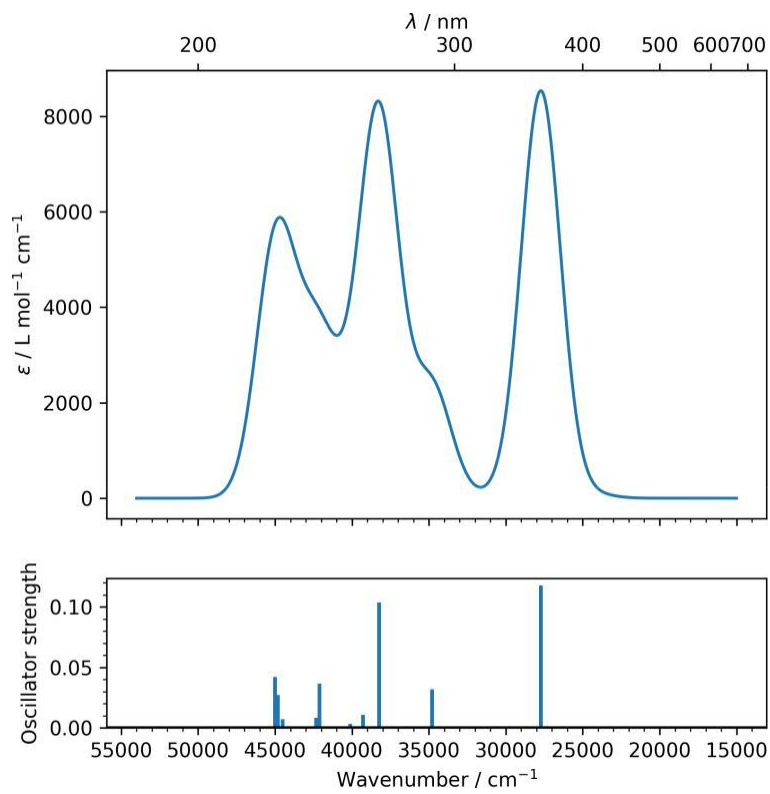


Fig. S17 Calculated UV-vis absorption spectrum of axial (S)-**1** with a gaussian broadening (FWHM = 3000 cm^{-1}).

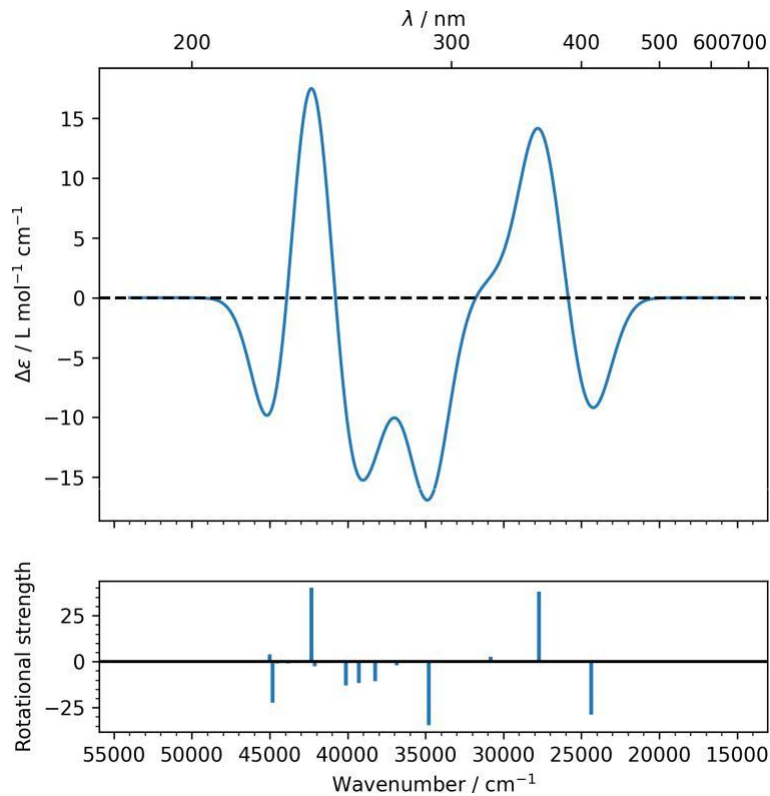


Fig. S18 Calculated CD spectrum of axial (S)-**1** with a gaussian broadening (FWHM = 3000 cm^{-1}).

Compound (*R*)-1, equatorial conformation

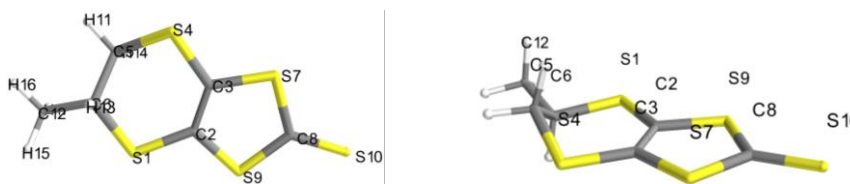


Fig. S19 Two views of the optimized geometry of equatorial (*R*)-1 together with the atom numbering scheme.

Total molecular energy	-2222.32580 hartrees
HOMO number	61
LUMO+1 energies	-0.84 eV
LUMO energies	-1.91 eV
HOMO energies	-5.97 eV
HOMO-1 energies	-6.59 eV
Geometry optimization specific results	
Converged nuclear repulsion energy	1119.80388 Hartrees
Frequency and Thermochemistry specific results	
Number of negative frequencies	0
Sum of electronic and zero-point energy	-2222.21652 Hartrees
Sum of electronic and thermal energies at 298.15 K	-2222.20492 Hartrees
Enthalpy at 298.15 K	-2222.20397 Hartrees
Gibbs free energy at 298.15 K	-2222.25571 Hartrees
Entropy at 298.15 K	0.00017 Hartrees

E.S.	Symmetry	Calculated mono-electronic excitations						
		nm	cm ⁻¹	f	R	Lambda	dCT	qCT Excitation description in %
1	Singlet-A	409	24400	0.001	-28.348	0.47	115.68	0.7560->62 (95) 61->62 (3)
2	Singlet-A	361	27680	0.119	36.575	0.60	295.95	0.6159->62 (2) 60->62 (3) 61->62 (92)
3	Singlet-A	323	30888	0.001	3.038	0.51	28.77	0.7061->63 (91) 61->64 (7)
4	Singlet-A	290	34448	0.031	-33.464	0.62	180.54	0.5258->62 (4) 61->63 (7) 61->64 (81) 61->66 (3)
5	Singlet-A	271	36775	0.001	-0.329	0.35	286.22	0.7958->62 (7) 60->63 (85) 60->64 (5)
6	Singlet-A	269	37061	0.001	0.024	0.48	237.11	0.7359->65 (2) 61->65 (94)
7	Singlet-A	261	38234	0.101	-8.291	0.58	300.47	0.5459->62 (90)
8	Singlet-A	255	39146	0.004	-7.164	0.41	247.21	0.5558->62 (66) 59->64 (2) 60->63 (3) 60->64 (4) 61->66 (19)
9	Singlet-A	249	40032	0.001	-6.364	0.25	458.99	0.8560->63 (6) 60->64 (87) 61->66 (2)
10	Singlet-A	239	41673	0.058	26.572	0.48	160.14	0.4758->62 (19) 59->64 (7) 61->64 (7) 61->66 (55)
11	Singlet-A	235	42396	0.000	2.728	0.42	16.49	0.7559->63 (91) 59->64 (3)
12	Singlet-A	227	44036	0.001	-1.031	0.46	174.60	0.6957->63 (2) 58->63 (83) 58->64 (2) 59->65 (4)
13	Singlet-A	224	44591	0.022	-10.314	0.49	201.81	0.6658->64 (5) 59->63 (2) 59->64 (78) 61->66 (9)
14	Singlet-A	220	45346	0.014	-0.023	0.31	470.47	0.6760->65 (49) 61->67 (40)
15	Singlet-A	220	45416	0.039	6.899	0.34	453.94	0.6660->65 (44) 61->67 (43) 61->68 (4)

Atomic charges population analysis. Selection of the most charged atoms based on Hirshfeld analysis

Atom and N°	Hirshfeld charge	CM5 charge	Mulliken charge
-------------	------------------	------------	-----------------

C 12	-0.250	-0.104	-0.386
S 10	-0.182	-0.199	-0.136
C 5	-0.148	-0.060	-0.363
H 11	+0.119	+0.062	+0.168
S 9	+0.126	+0.099	+0.220

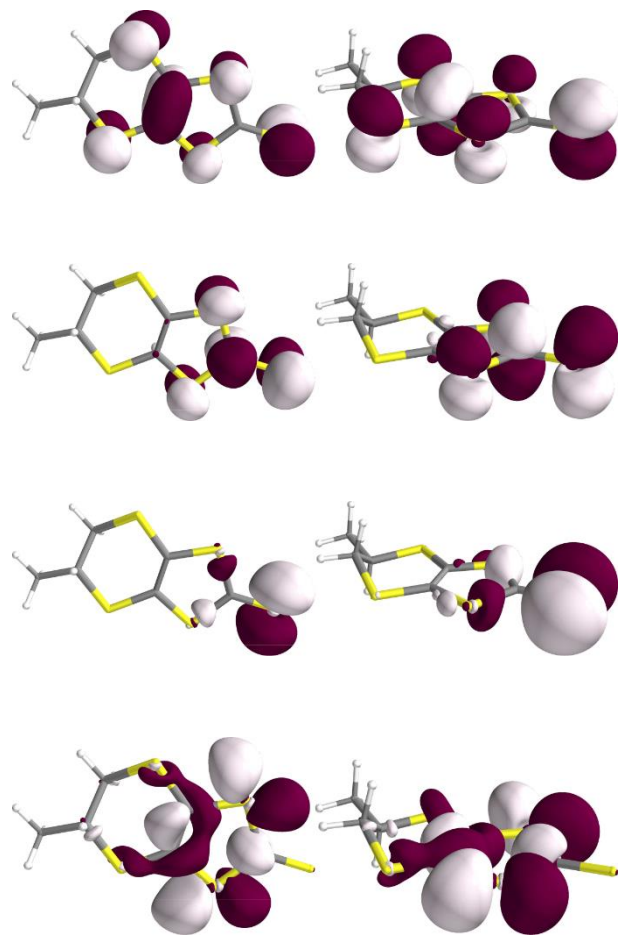


Fig. S20 HOMO, LUMO, HOMO-1 and LUMO+1 (from top to bottom, two views each) of equatorial (R)-1.

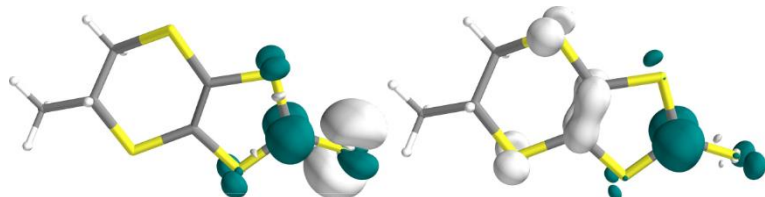


Fig. S21 Representation of the Electron Density Difference (S1-S0 left) and (S2-S0 right) of equatorial (R)-1. The excited electron and hole regions are indicated by respectively blue and white surfaces.

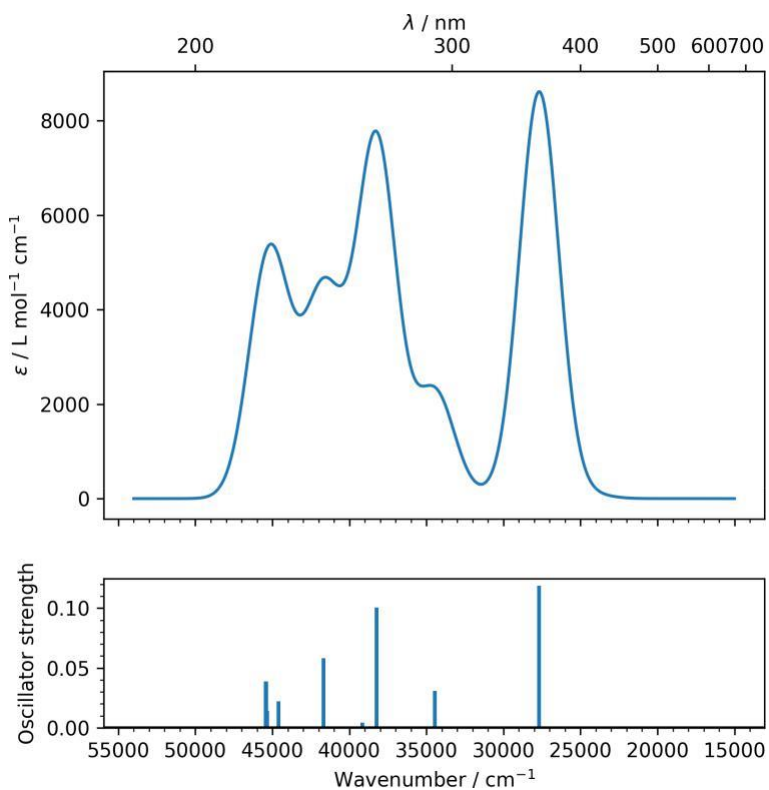


Fig. S22 Calculated UV-vis absorption spectrum of equatorial (R)-**1** with a gaussian broadening (FWHM = 3000 cm^{-1}).

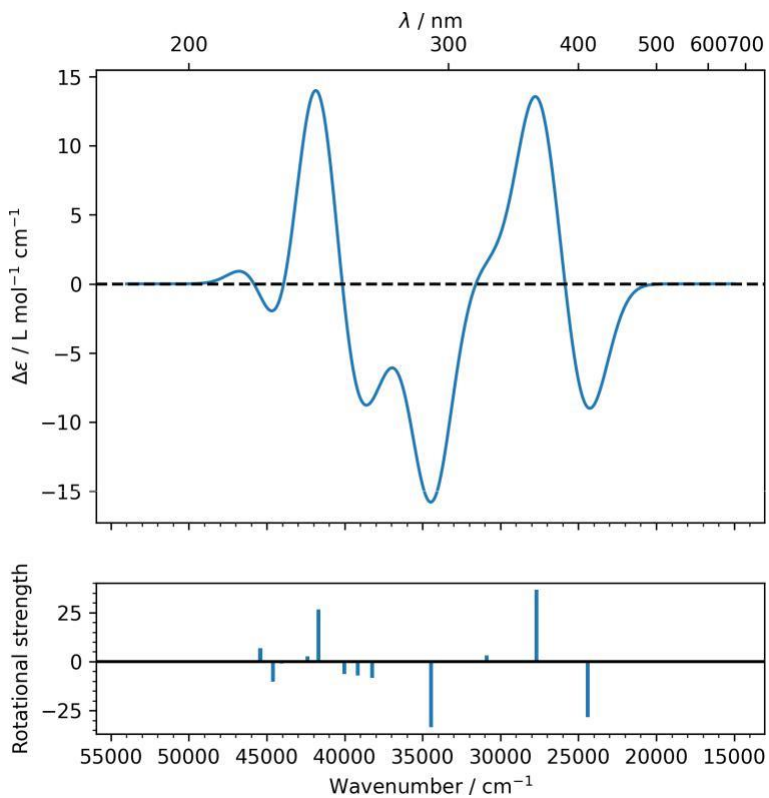


Fig. S23 Calculated CD spectrum of equatorial (R)-**1** with a gaussian broadening (FWHM = 3000 cm^{-1}).

Compound (S)-1, equatorial conformation

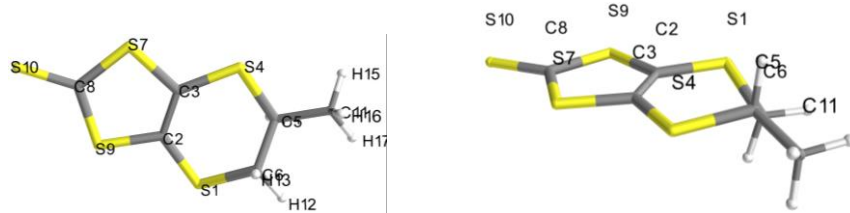


Fig. S24 Two views of the optimized geometry of equatorial (S)-1 together with the atom numbering scheme.

Total molecular energy	-2222.32580 hartrees
HOMO number	61
LUMO+1 energies	-0.84 eV
LUMO energies	-1.91 eV
HOMO energies	-5.97 eV
HOMO-1 energies	-6.59 eV
Geometry optimization specific results	
Converged nuclear repulsion energy	1119.80413 Hartrees
Frequency and Thermochemistry specific results	
Number of negative frequencies	0
Sum of electronic and zero-point energy	-2222.21652 Hartrees
Sum of electronic and thermal energies at 298.15 K	-2222.20492 Hartrees
Enthalpy at 298.15 K	-2222.20397 Hartrees
Gibbs free energy at 298.15 K	-2222.25572 Hartrees
Entropy at 298.15 K	0.00017 Hartrees

Calculated mono-electronic excitations										
E.S.	Symmetry	nm	cm-1	f	R	Lambda	dCT	qCT	Excitation description in %	
1	Singlet-A	409	24401	0.001	28.338	0.47	115.69	0.75	60->62 (95) 61->62 (3)	
2	Singlet-A	361	27680	0.119	-36.548	0.60	295.97	0.61	59->62 (2) 60->62 (3) 61->62 (92)	
3	Singlet-A	323	30889	0.001	-3.041	0.51	28.80	0.70	61->63 (91) 61->64 (7)	
4	Singlet-A	290	34451	0.031	33.450	0.62	180.51	0.52	58->62 (4) 61->63 (7) 61->64 (81) 61->66 (3)	
5	Singlet-A	271	36776	0.001	0.327	0.35	286.15	0.79	58->62 (7) 60->63 (85) 60->64 (5)	
6	Singlet-A	269	37062	0.001	-0.050	0.48	237.26	0.73	59->65 (2) 61->65 (94)	
7	Singlet-A	261	38234	0.101	8.278	0.58	300.50	0.54	59->62 (90)	
8	Singlet-A	255	39146	0.004	7.175	0.41	247.30	0.55	58->62 (66) 59->64 (2) 60->63 (3) 60->64 (4) 61->66 (19)	
9	Singlet-A	249	40034	0.001	6.361	0.25	458.98	0.85	60->63 (6) 60->64 (87) 61->66 (2)	
10	Singlet-A	239	41673	0.058	-26.543	0.48	160.30	0.47	58->62 (19) 59->64 (6) 61->64 (7) 61->66 (55)	
11	Singlet-A	235	42397	0.000	-2.733	0.42	16.56	0.75	59->63 (91) 59->64 (3)	
12	Singlet-A	227	44037	0.001	1.038	0.46	174.69	0.69	57->63 (2) 58->63 (83) 58->64 (2) 59->65 (4)	
13	Singlet-A	224	44593	0.022	10.311	0.49	201.72	0.66	58->64 (5) 59->63 (2) 59->64 (78) 61->66 (9)	
14	Singlet-A	220	45346	0.013	0.048	0.32	464.48	0.67	60->65 (47) 61->67 (42)	
15	Singlet-A	220	45416	0.040	-6.913	0.33	460.66	0.67	60->65 (46) 61->67 (41) 61->68 (4)	

Atomic charges population analysis. Selection of the most charged atoms based on Hirshfeld analysis			
Atom and N°	Hirshfeld charge	CM5 charge	Mulliken charge
C 11	-0.250	-0.104	-0.386
S 10	-0.182	-0.199	-0.136
C 6	-0.148	-0.060	-0.363
H 12	+0.119	+0.062	+0.168

S 9

+0.127

+0.099

+0.226

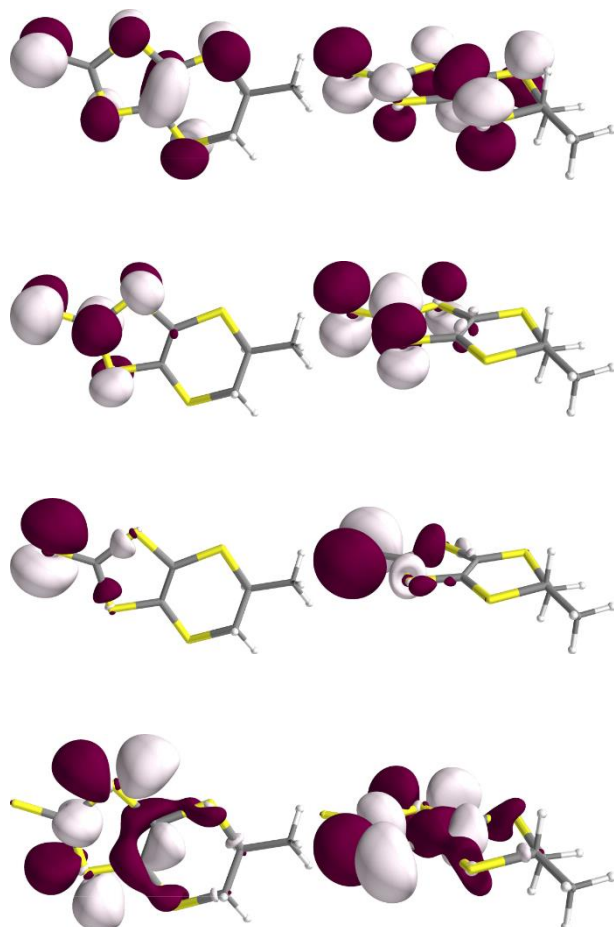


Fig. S25 HOMO, LUMO, HOMO-1 and LUMO+1 (from top to bottom, two views each) of equatorial (*S*)-1.

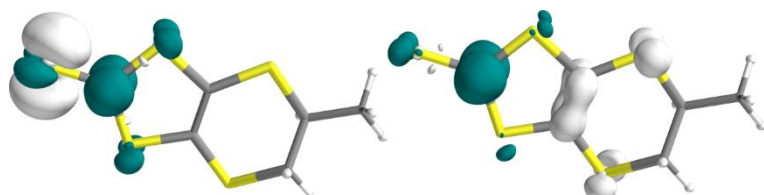


Fig. S26 Representation of the Electron Density Difference (S1-S0 left) and (S2-S0 right) of equatorial (*S*)-1. The excited electron and hole regions are indicated by respectively blue and white surfaces.

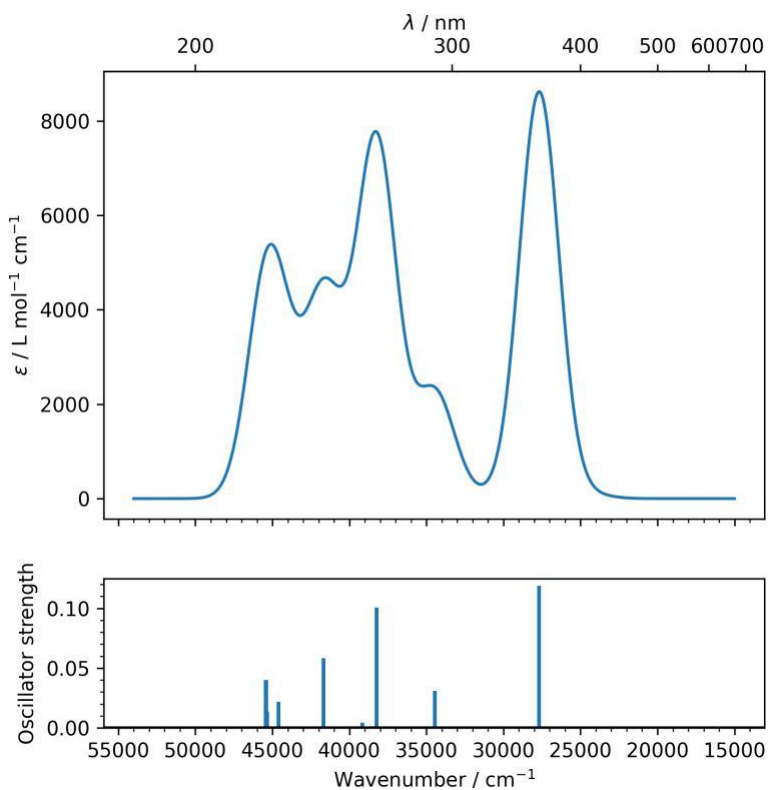


Fig. S27 Calculated UV-vis absorption spectrum of equatorial (S)-**1** with a gaussian broadening (FWHM = 3000 cm^{-1}).

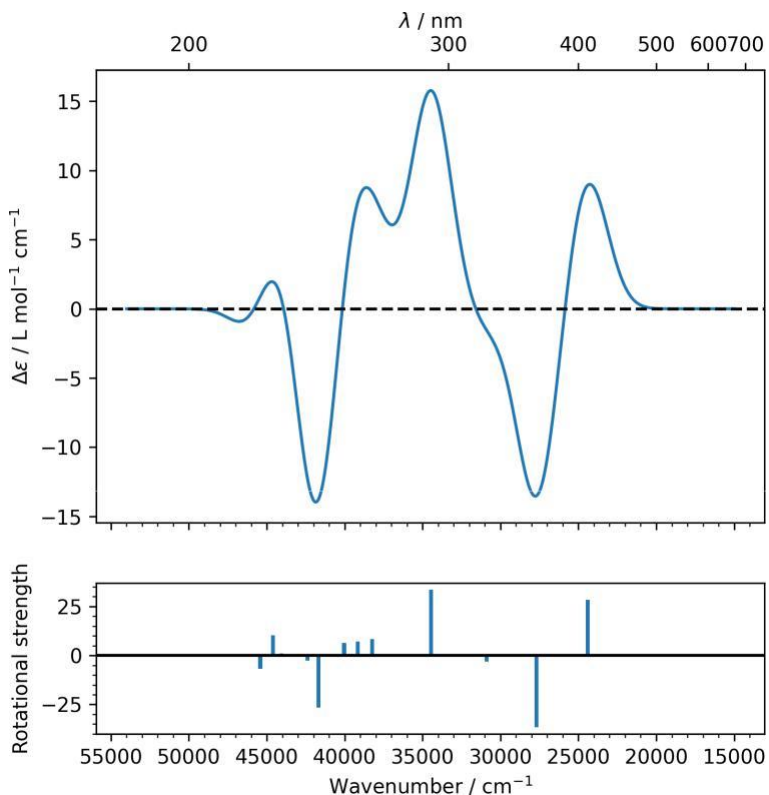


Fig. S28 Calculated CD spectrum of equatorial (S)-**1** with a gaussian broadening (FWHM = 3000 cm^{-1}).

Compound (*R,R*)-2, axial conformation

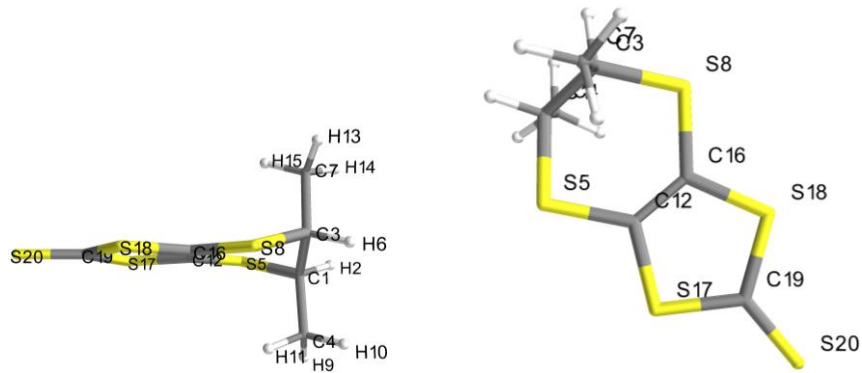


Fig. S29 Two views of the optimized geometry of axial (*R,R*)-2 together with the atom numbering scheme.

Total molecular energy	-2261.60481 hartrees
HOMO number	65
LUMO+1 energies	-0.83 eV
LUMO energies	-1.89 eV
HOMO energies	-5.96 eV
HOMO-1 energies	-6.57 eV

Geometry optimization specific results

Converged nuclear repulsion energy	1275.57674 Hartrees
------------------------------------	---------------------

Frequency and Thermochemistry specific results

Number of negative frequencies	0
Sum of electronic and zero-point energy	-2261.46753 Hartrees
Sum of electronic and thermal energies at 298.15 K	-2261.45455 Hartrees
Enthalpy at 298.15 K	-2261.45361 Hartrees
Gibbs free energy at 298.15 K	-2261.50809 Hartrees
Entropy at 298.15 K	0.00018 Hartrees

Calculated mono-electronic excitations									
E.S.	Symmetry	nm	cm-1	f	R	Lambda	dCT	qCT	Excitation description in %
1	Singlet-A	410	24359	0.001	28.177	0.47	116.18	0.76	64->66 (95) 65->66 (3)
2	Singlet-A	360	27727	0.121	-36.643	0.60	297.24	0.61	63->66 (2) 64->66 (3) 65->66 (92)
3	Singlet-A	324	30860	0.001	-2.202	0.48	53.29	0.75	65->67 (98)
4	Singlet-A	281	35564	0.028	29.191	0.65	141.86	0.47	62->66 (10) 65->68 (83) 65->70 (2)
5	Singlet-A	272	36677	0.002	2.099	0.36	264.33	0.79	62->66 (6) 64->67 (91)
6	Singlet-A	272	36757	0.001	0.749	0.48	243.17	0.74	63->69 (2) 65->69 (95)
7	Singlet-A	261	38248	0.108	8.651	0.61	277.20	0.55	63->66 (92) 64->73 (3)
8	Singlet-A	254	39229	0.015	19.696	0.40	293.81	0.57	62->66 (70) 64->67 (6) 64->68 (2) 65->68 (4) 65->70 (11)
9	Singlet-A	245	40651	0.001	10.564	0.22	442.16	0.88	64->68 (95)
10	Singlet-A	236	42198	0.026	20.334	0.47	101.66	0.60	62->66 (5) 63->67 (46) 63->68 (5) 65->68 (4) 65->70 (29) 65->71 (3) 65->72 (2)
11	Singlet-A	235	42373	0.021	-59.950	0.46	93.10	0.61	62->66 (4) 62->69 (3) 63->67 (48) 63->68 (3) 65->68 (4) 65->70 (27) 65->71 (4)
12	Singlet-A	229	43664	0.000	1.034	0.45	183.53	0.74	61->67 (2) 62->67 (89) 63->69 (4)
13	Singlet-A	226	44078	0.005	6.765	0.47	371.54	0.66	65->70 (12) 65->71 (40) 65->72 (42)
14	Singlet-A	222	44926	0.043	-3.800	0.24	522.67	0.87	64->69 (95)
15	Singlet-A	219	45542	0.026	35.839	0.51	212.65	0.64	63->68 (85) 65->70 (7) 65->71 (3)

Atomic charges population analysis. Selection of the most charged atoms based on Hirshfeld analysis

Atom and N° Hirshfeld charge CM5 charge

Mulliken charge

C 4	-0.262	-0.113	-0.297
C 7	-0.261	-0.113	-0.297
S 20	-0.183	-0.201	-0.138

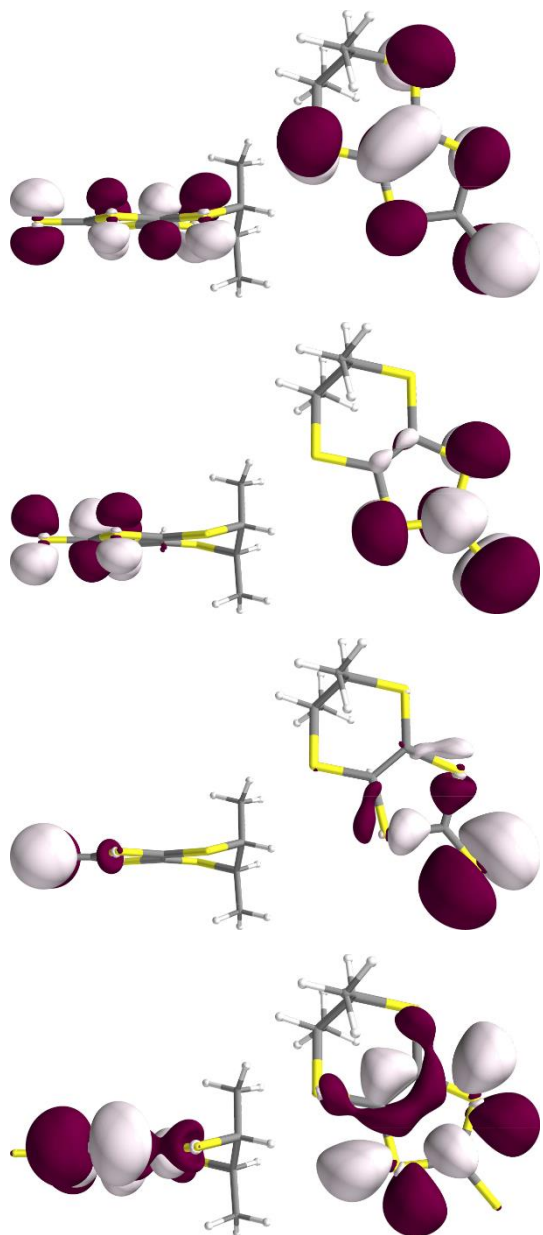


Fig. S30 HOMO, LUMO, HOMO-1 and LUMO+1 (from top to bottom, two views each) of axial (*R,R*)-2.

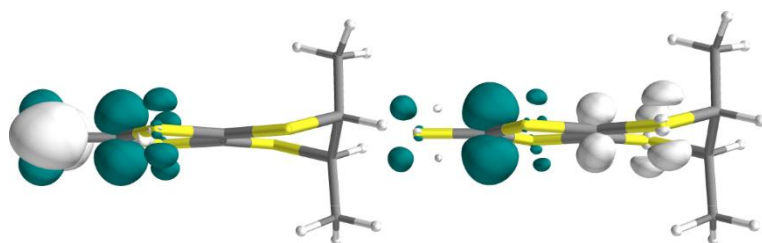


Fig. S31 Representation of the Electron Density Difference (S1-S0 left) and (S2-S0 right) of axial (*R,R*)-2. The excited electron and hole regions are indicated by respectively blue and white surfaces.

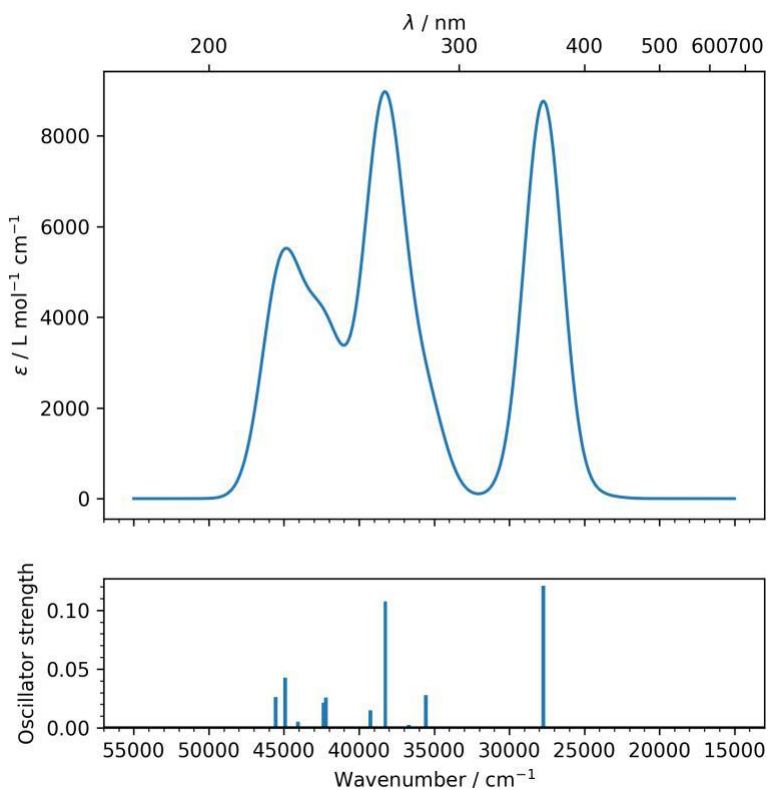


Fig. S32 Calculated UV-vis absorption spectrum of axial (*R,R*)-**2** with a gaussian broadening (FWHM = 3000 cm^{-1}).

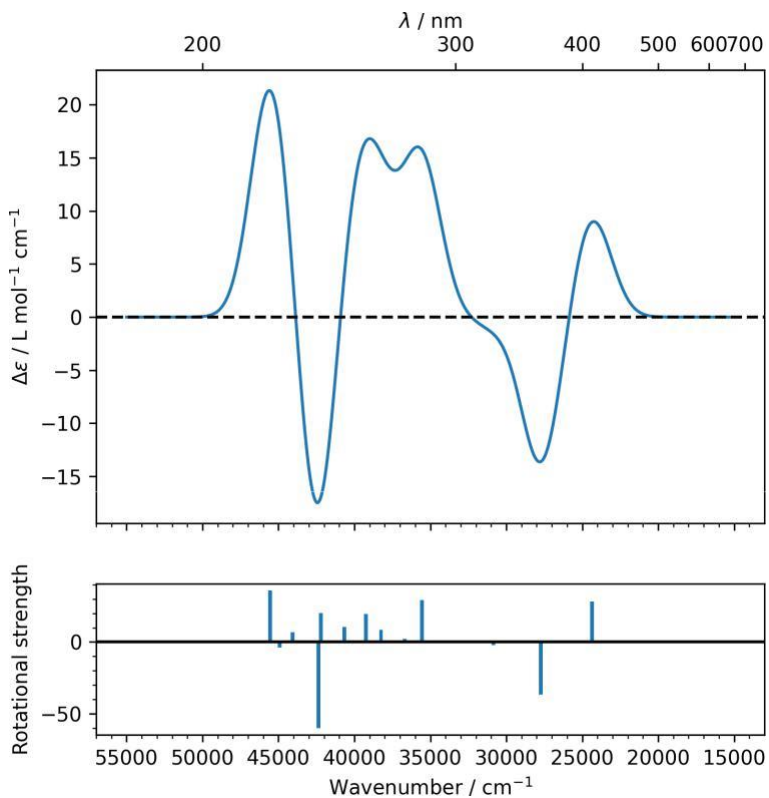


Fig. S33 Calculated CD spectrum of axial (*R,R*)-**2** with a gaussian broadening (FWHM = 3000 cm^{-1}).

Compound (S,S)-2, axial conformation

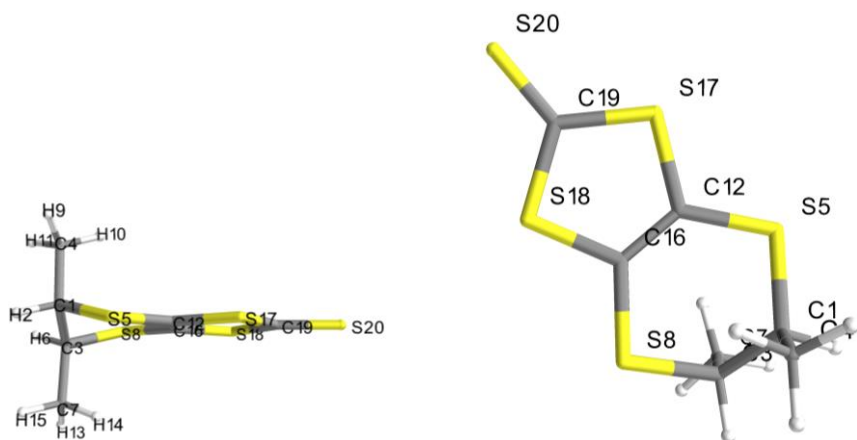


Fig. S34 Two views of the optimized geometry of axial (S,S)-2 together with the atom numbering scheme.

Total molecular energy	-2261.60481 hartrees
HOMO number	65
LUMO+1 energies	-0.83 eV
LUMO energies	-1.89 eV
HOMO energies	-5.96 eV
HOMO-1 energies	-6.57 eV

Geometry optimization specific results

Converged nuclear repulsion energy	1275.57484 Hartrees
------------------------------------	---------------------

Frequency and Thermochemistry specific results

Number of negative frequencies	0
Sum of electronic and zero-point energy	-2261.46753 Hartrees
Sum of electronic and thermal energies at 298.15 K	-2261.45455 Hartrees
Enthalpy at 298.15 K	-2261.45361 Hartrees
Gibbs free energy at 298.15 K	-2261.50808 Hartrees
Entropy at 298.15 K	0.00018 Hartrees

E.S.	Symmetry	Calculated mono-electronic excitations							
		nm	cm-1	f	R	Lambda	dCT	qCT	Excitation description in %
1	Singlet-A	410	24359	0.001	-28.178	0.47	116.18	0.76	64->66 (95) 65->66 (3)
2	Singlet-A	360	27727	0.121	36.643	0.60	297.24	0.61	63->66 (2) 64->66 (3) 65->66 (92)
3	Singlet-A	324	30860	0.001	2.203	0.48	53.30	0.75	65->67 (98)
4	Singlet-A	281	35564	0.028	-29.194	0.65	141.86	0.47	62->66 (10) 65->68 (83) 65->70 (2)
5	Singlet-A	272	36677	0.002	-2.098	0.36	264.32	0.79	62->66 (6) 64->67 (91)
6	Singlet-A	272	36757	0.001	-0.749	0.48	243.17	0.74	63->69 (2) 65->69 (95)
7	Singlet-A	261	38248	0.108	-8.650	0.61	277.20	0.55	63->66 (92) 64->73 (3)
8	Singlet-A	254	39229	0.015	-19.695	0.40	293.79	0.57	62->66 (70) 64->67 (6) 64->68 (2) 65->68 (4) 65->70 (11)
9	Singlet-A	245	40651	0.001	-10.563	0.22	442.16	0.88	64->68 (95)
10	Singlet-A	236	42197	0.026	-20.320	0.47	101.77	0.60	62->66 (5) 63->67 (46) 63->68 (5) 65->68 (4) 65->70 (29) 65->71 (3) 65->72 (2)
11	Singlet-A	236	42372	0.021	59.934	0.46	92.96	0.61	62->66 (4) 62->69 (3) 63->67 (48) 63->68 (3) 65->68 (4) 65->70 (27) 65->71 (4)
12	Singlet-A	229	43664	0.000	-1.033	0.45	183.52	0.74	61->67 (2) 62->67 (89) 63->69 (4)
13	Singlet-A	226	44078	0.005	-6.765	0.47	371.53	0.66	65->70 (12) 65->71 (40) 65->72 (42)
14	Singlet-A	222	44926	0.043	3.801	0.24	522.67	0.87	64->69 (95)

15 Singlet-A 219 45542 0.026 -35.837 0.51 212.65 0.64 63->68 (85) 65->70 (7) 65->71 (3)

Atomic charges population analysis. Selection of the most charged atoms based on Hirshfeld analysis

Atom and N° Hirshfeld charge CM5 charge

Mulliken charge

C 4	-0.262	-0.113	-0.297
C 7	-0.261	-0.113	-0.297
S 20	-0.183	-0.201	-0.138

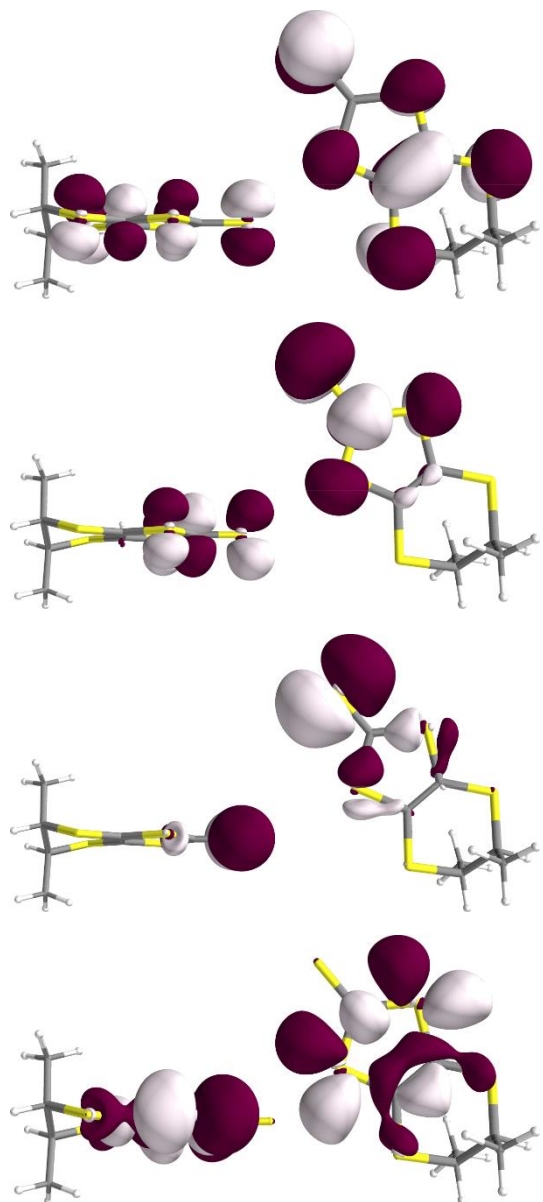


Fig. S35 HOMO, LUMO, HOMO-1 and LUMO+1 (from top to bottom, two views each) of axial (S,S)-2.

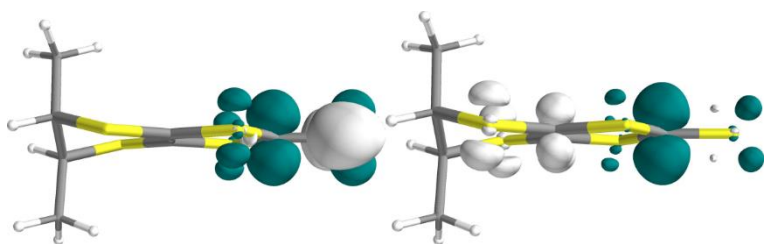


Fig. S36 Representation of the Electron Density Difference (S_1-S_0 left) and (S_2-S_0 right) of axial (S,S)-2. The excited electron and hole regions are indicated by respectively blue and white surfaces.

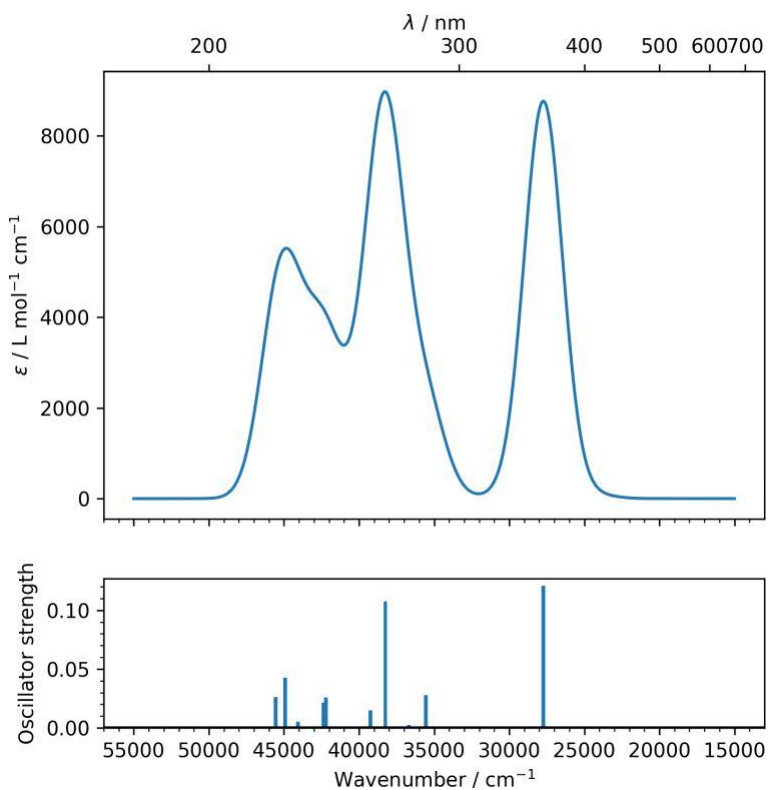


Fig. S37 Calculated UV-vis absorption spectrum of axial (S,S)-**2** with a gaussian broadening (FWHM = 3000 cm^{-1}).

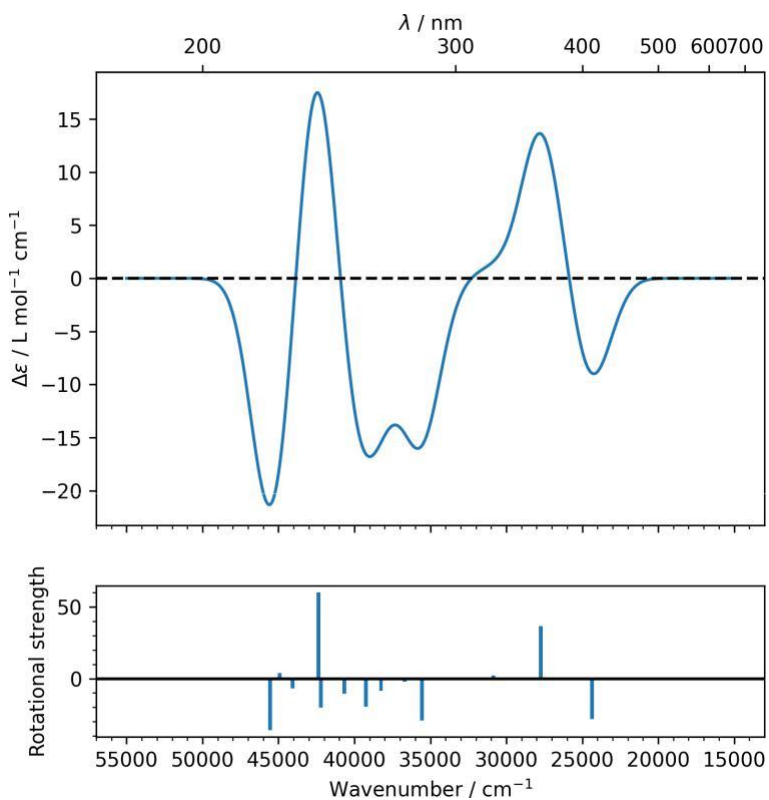


Fig. S38 Calculated CD spectrum of axial (S,S)-**2** with a gaussian broadening (FWHM = 3000 cm^{-1}).

Compound (*R,R*)-2, equatorial conformation

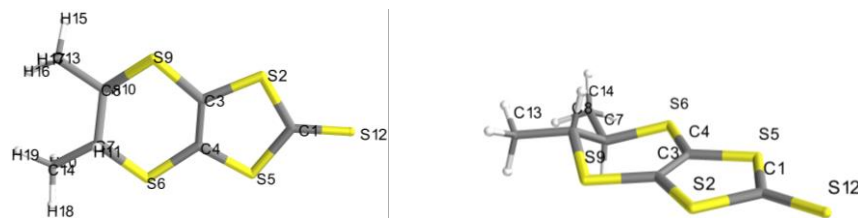


Fig. S39 Two views of the optimized geometry of equatorial (*R,R*)-2 together with the atom numbering scheme.

Total molecular energy	-2261.60306 hartrees
HOMO number	65
LUMO+1 energies	-0.79 eV
LUMO energies	-1.87 eV
HOMO energies	-5.91 eV
HOMO-1 energies	-6.56 eV
Geometry optimization specific results	
Converged nuclear repulsion energy	1250.94798 Hartrees
Frequency and Thermochemistry specific results	
Number of negative frequencies	1
Sum of electronic and zero-point energy	-2261.46578 Hartrees
Sum of electronic and thermal energies at 298.15 K	-2261.45359 Hartrees
Enthalpy at 298.15 K	-2261.45264 Hartrees
Gibbs free energy at 298.15 K	-2261.50459 Hartrees
Entropy at 298.15 K	0.00017 Hartrees

Calculated mono-electronic excitations									
E.S.	Symmetry	nm	cm-1	f	R	Lambda	dCT	qCT	Excitation description in %
1	Singlet-A	409	24405	0.002	-32.603	0.47	113.54	0.75	64->66 (95) 65->66 (4)
2	Singlet-A	364	27408	0.118	41.495	0.59	299.73	0.62	63->66 (2) 64->66 (4) 65->66 (92)
3	Singlet-A	324	30778	0.001	3.388	0.54	11.68	0.67	65->67 (85) 65->68 (13)
4	Singlet-A	293	34015	0.027	-37.842	0.61	148.50	0.54	62->66 (3) 65->67 (12) 65->68 (75) 65->70 (4)
5	Singlet-A	271	36853	0.001	0.037	0.35	302.05	0.78	62->66 (8) 64->67 (79) 64->68 (10)
6	Singlet-A	267	37413	0.003	-2.359	0.47	217.55	0.71	63->69 (2) 65->69 (92)
7	Singlet-A	262	38152	0.105	-7.408	0.60	267.28	0.53	63->66 (90) 64->72 (2)
8	Singlet-A	257	38818	0.000	-0.373	0.43	155.07	0.53	62->66 (55) 63->68 (2) 64->67 (4) 64->68 (2) 65->70 (32)
9	Singlet-A	249	40113	0.001	-0.632	0.27	449.38	0.84	64->67 (10) 64->68 (83) 65->70 (3)
10	Singlet-A	242	41172	0.069	24.023	0.46	73.36	0.46	62->66 (30) 63->68 (2) 64->67 (3) 65->68 (7) 65->70 (46)
11	Singlet-A	236	42359	0.000	-3.931	0.44	20.42	0.75	63->67 (88) 63->68 (8)
12	Singlet-A	226	44058	0.001	0.961	0.48	158.46	0.69	61->67 (2) 62->67 (82) 62->68 (5) 63->69 (4)
13	Singlet-A	224	44460	0.017	-10.787	0.48	191.10	0.67	63->67 (6) 63->68 (82) 65->70 (5)
14	Singlet-A	223	44733	0.007	1.325	0.48	329.22	0.69	65->71 (91) 65->73 (3)
15	Singlet-A	217	45900	0.020	-0.945	0.48	119.36	0.61	62->68 (67) 62->70 (2) 63->69 (7) 64->69 (13)

Atomic charges population analysis. Selection of the most charged atoms based on Hirshfeld analysis			
Atom and N°	Hirshfeld charge	CM5 charge	Mulliken charge
C 14	-0.251	-0.105	-0.431
C 13	-0.251	-0.105	-0.430
S 12	-0.184	-0.201	-0.138
S 5	+0.126	+0.099	+0.219

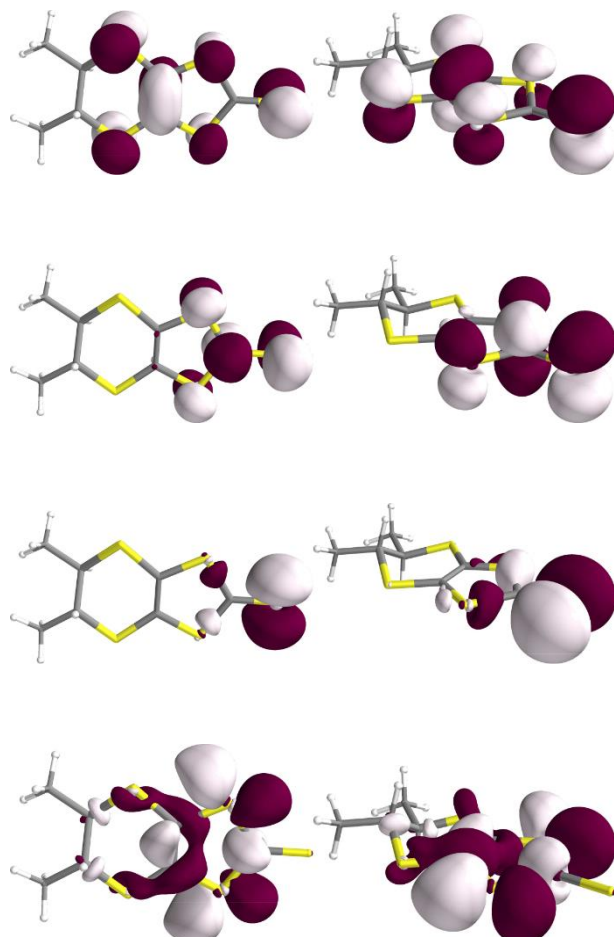


Fig. S40 HOMO, LUMO, HOMO-1 and LUMO+1 (from top to bottom, two views each) of equatorial (*R,R*)-**2**.

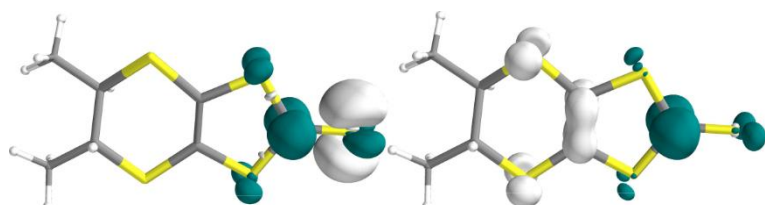


Fig. S41 Representation of the Electron Density Difference (S1-S0 left) and (S2-S0 right) of equatorial (*R,R*)-**2**. The excited electron and hole regions are indicated by respectively blue and white surfaces.

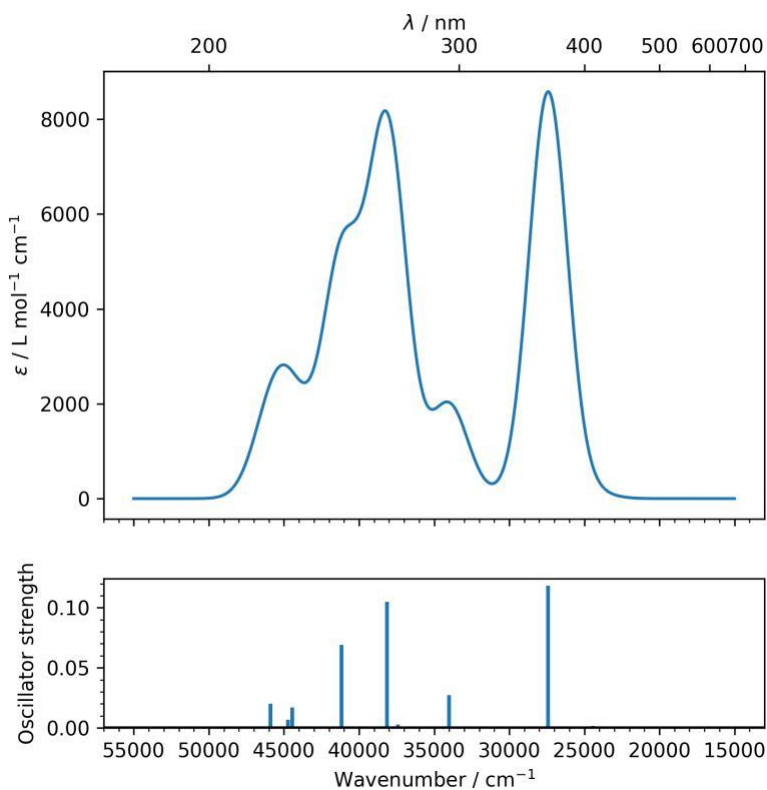


Fig. S42 Calculated UV-vis absorption spectrum of equatorial (*R,R*)-**2** with a gaussian broadening (FWHM = 3000 cm^{-1}).

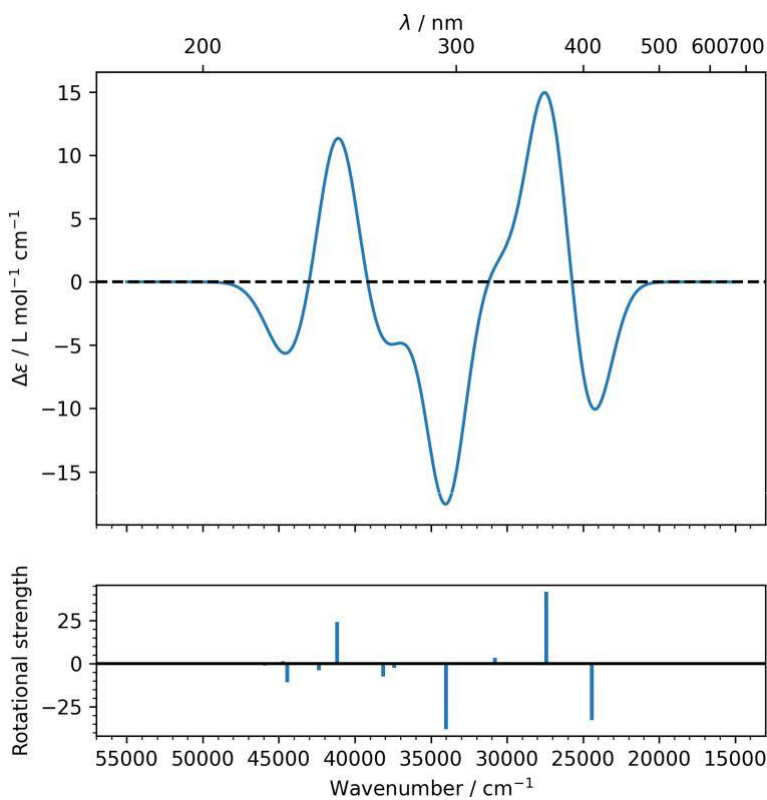


Fig. S43 Calculated CD spectrum of equatorial (*R,R*)-**2** with a gaussian broadening (FWHM = 3000 cm^{-1}).

Compound (S,S)-2, equatorial conformation

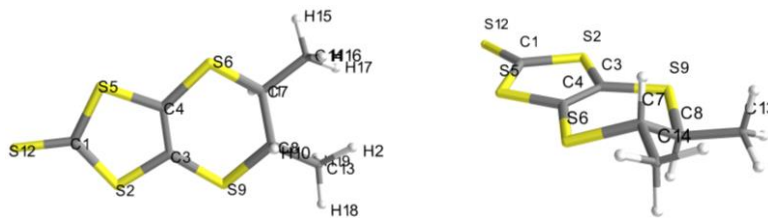


Fig. S44 Two views of the optimized geometry of equatorial (S,S)-2 together with the atom numbering scheme.

Total molecular energy	-2261.60307 hartrees
HOMO number	65
LUMO+1 energies	-0.79 eV
LUMO energies	-1.87 eV
HOMO energies	-5.91 eV
HOMO-1 energies	-6.56 eV
Geometry optimization specific results	
Converged nuclear repulsion energy	1250.99903 Hartrees
Frequency and Thermochemistry specific results	
Number of negative frequencies	1
Sum of electronic and zero-point energy	-2261.46578 Hartrees
Sum of electronic and thermal energies at 298.15 K	-2261.45359 Hartrees
Enthalpy at 298.15 K	-2261.45265 Hartrees
Gibbs free energy at 298.15 K	-2261.50460 Hartrees
Entropy at 298.15 K	0.00017 Hartrees

Calculated mono-electronic excitations								
E.S.	Symmetry	nm	cm ⁻¹	f	R	Lambda	dCT	qCT Excitation description in %
1	Singlet-A	409	24406	0.002	31.979	0.47	113.91	0.75 64->66 (95) 65->66 (4)
2	Singlet-A	364	27423	0.119	-40.618	0.59	299.96	0.62 63->66 (2) 64->66 (4) 65->66 (92)
3	Singlet-A	324	30803	0.001	-3.323	0.53	14.24	0.68 65->67 (85) 65->68 (12)
4	Singlet-A	293	34064	0.028	37.420	0.61	150.16	0.53 62->66 (3) 65->67 (12) 65->68 (76) 65->70 (3)
5	Singlet-A	271	36857	0.001	-0.060	0.35	299.29	0.78 62->66 (8) 64->67 (80) 64->68 (10)
6	Singlet-A	267	37415	0.003	0.998	0.46	246.52	0.70 65->69 (89) 65->70 (3)
7	Singlet-A	262	38152	0.104	7.602	0.60	268.58	0.53 63->66 (90) 64->72 (2)
8	Singlet-A	257	38832	0.000	0.839	0.43	162.46	0.53 62->66 (55) 63->68 (2) 64->67 (4) 64->68 (2) 65->70 (31)
9	Singlet-A	249	40120	0.001	0.803	0.27	450.10	0.84 64->67 (9) 64->68 (83) 65->70 (3)
10	Singlet-A	242	41167	0.068	-23.019	0.46	83.72	0.47 62->66 (30) 63->68 (2) 64->67 (3) 65->68 (7) 65->69 (2) 65->70 (45)
11	Singlet-A	235	42374	0.000	3.430	0.44	18.33	0.75 63->67 (88) 63->68 (8)
12	Singlet-A	226	44067	0.001	-0.341	0.48	154.37	0.69 61->67 (2) 62->67 (80) 62->68 (4) 63->68 (2) 63->69 (4)
13	Singlet-A	224	44466	0.016	10.492	0.49	177.80	0.68 62->67 (2) 62->68 (3) 63->67 (6) 63->68 (79) 65->70 (5)
14	Singlet-A	223	44697	0.006	-1.288	0.48	329.81	0.69 65->71 (91) 65->73 (3)
15	Singlet-A	217	45944	0.015	1.084	0.44	149.20	0.58 62->68 (62) 63->69 (5) 64->69 (16)

Atomic charges population analysis. Selection of the most charged atoms based on Hirshfeld analysis
 Atom and N° Hirshfeld charge CM5 charge Mulliken charge

C 13	-0.251	-0.105	-0.431
C 14	-0.251	-0.105	-0.430
S 12	-0.184	-0.201	-0.138
S 5	+0.126	+0.098	+0.222

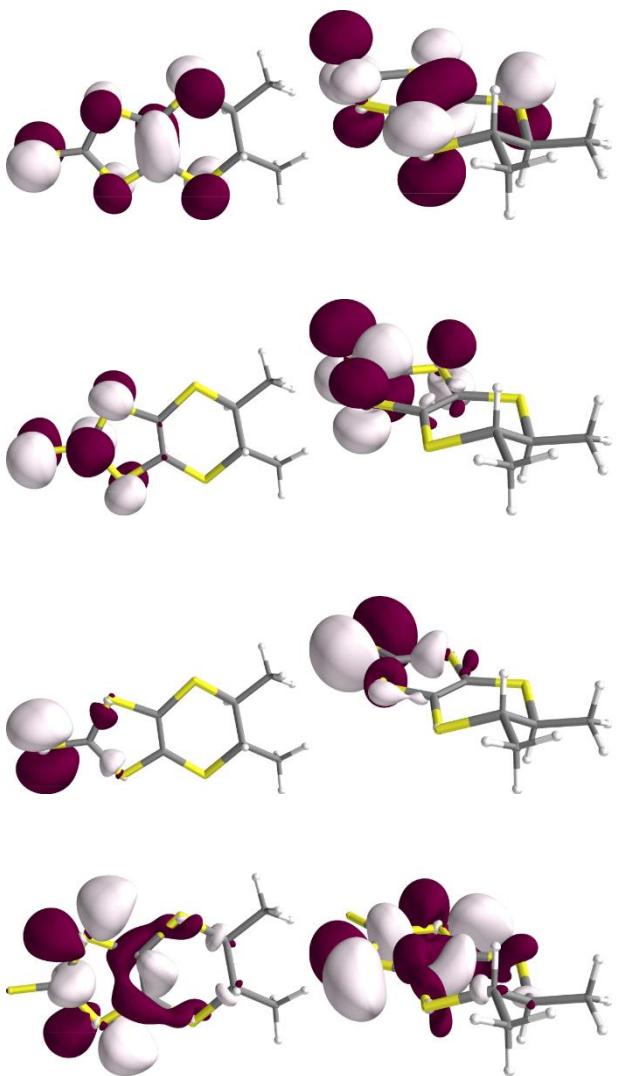


Fig. S45 HOMO, LUMO, HOMO-1 and LUMO+1 (from top to bottom, two views each) of equatorial (*S,S*)-**2**.

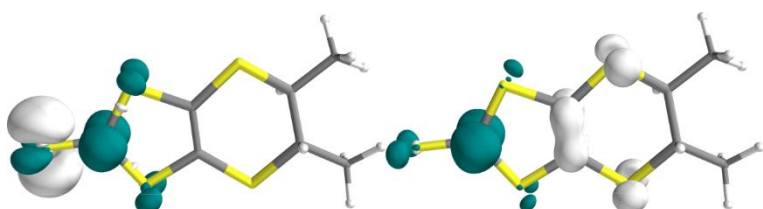


Fig. S46 Representation of the Electron Density Difference (S1-S0 left) and (S2-S0 right) of equatorial (*S,S*)-**2**. The excited electron and hole regions are indicated by respectively blue and white surfaces.

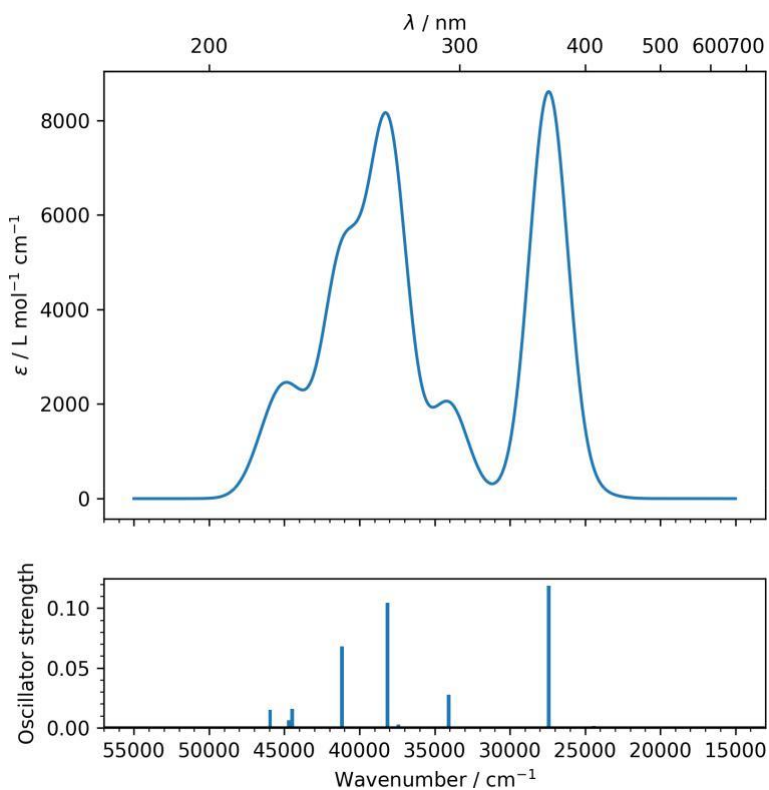


Fig. S47 Calculated UV-vis absorption spectrum of equatorial (S,S)-2 with a gaussian broadening (FWHM = 3000 cm^{-1}).

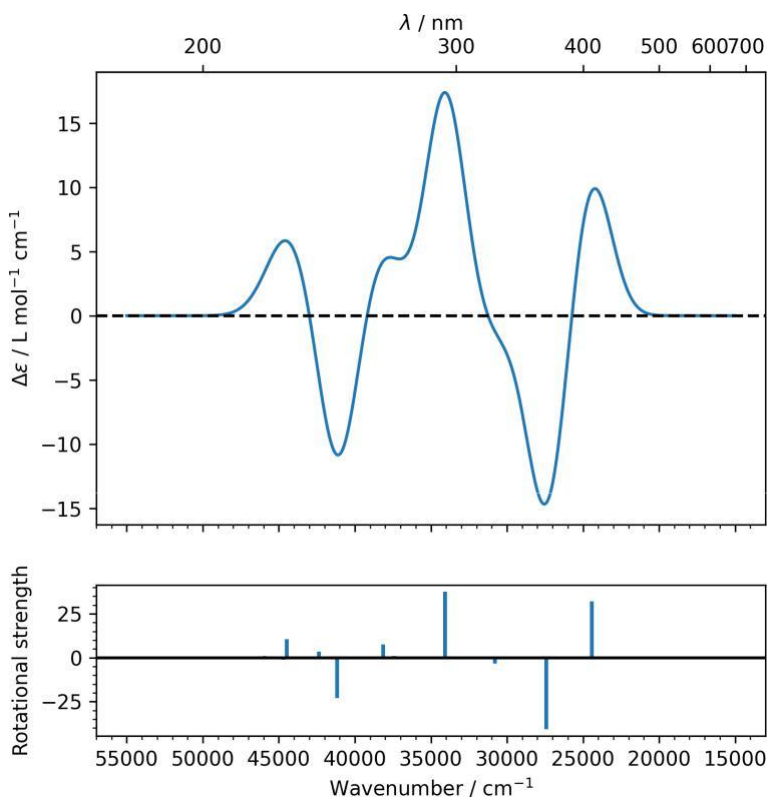
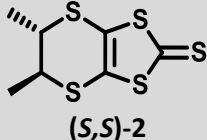
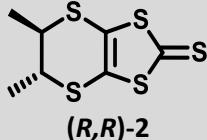
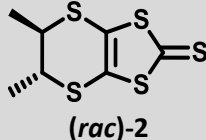


Fig. S48 Calculated CD spectrum of equatorial (S,S)-2 with a gaussian broadening (FWHM = 3000 cm^{-1}).

Table S1 Crystallographic data for (*S,S*)-, (*R,R*)- and (*rac*)-dm-dddt-thione **2**

			
Empirical formula	C ₇ H ₈ S ₅	C ₇ H ₈ S ₅	C ₇ H ₈ S ₅
Fw	252.43	252.43	252.43
Crystal color	Yellow	Yellow	Yellow
Crystal size (mm ³)	0.40*0.07*0.03	0.40*0.04*0.02	0.11*0.08*0.06
Temperature (K)	150	150	150
Wavelength (Å)	1.54154	1.54184	1.54184
Crystal system, Z	Monoclinic, 4	Monoclinic, 4	Monoclinic, 4
Space group	P2 ₁	P2 ₁	P2 ₁ /n
a (Å)	7.4413(2)	7.4434(2)	13.2577 (9)
b (Å)	15.6747(4)	15.6819(4)	5.9544 (4)
c (Å)	8.6991(2)	8.7048(2)	13.8006 (8)
α (°)	90	90	90
β (°)	92.916(2)	92.980(2)	106.797 (7)
γ (°)	90	90	90
V (Å ³)	1013.35(4)	1014.71(4)	1042.96 (12)
ρ _{calc} (g.cm ⁻³)	1.655	1.652	1.608
μ(CuKα) (mm ⁻¹)	10.060	10.046	9.774
θ range (°)	5.091–73.592	5.088–73.415	4.073–72.898
Data collected	6956	7411	3768
Data unique	3887	3915	2027
Data observed	3670	3581	1624
R(int)	0.0508	0.0561	0.0468
Nb of parameters / restraints	217/1	217/1	129/0
Flack parameter	0.07(5)	-0.08(3)	-
R1(F), ^a I > 2σ(I)	0.0449	0.0419	0.0444
wR2(F ²), ^b all data	0.1378	0.1153	0.1188
S(F ²), ^c all data	1.077	1.055	1.015

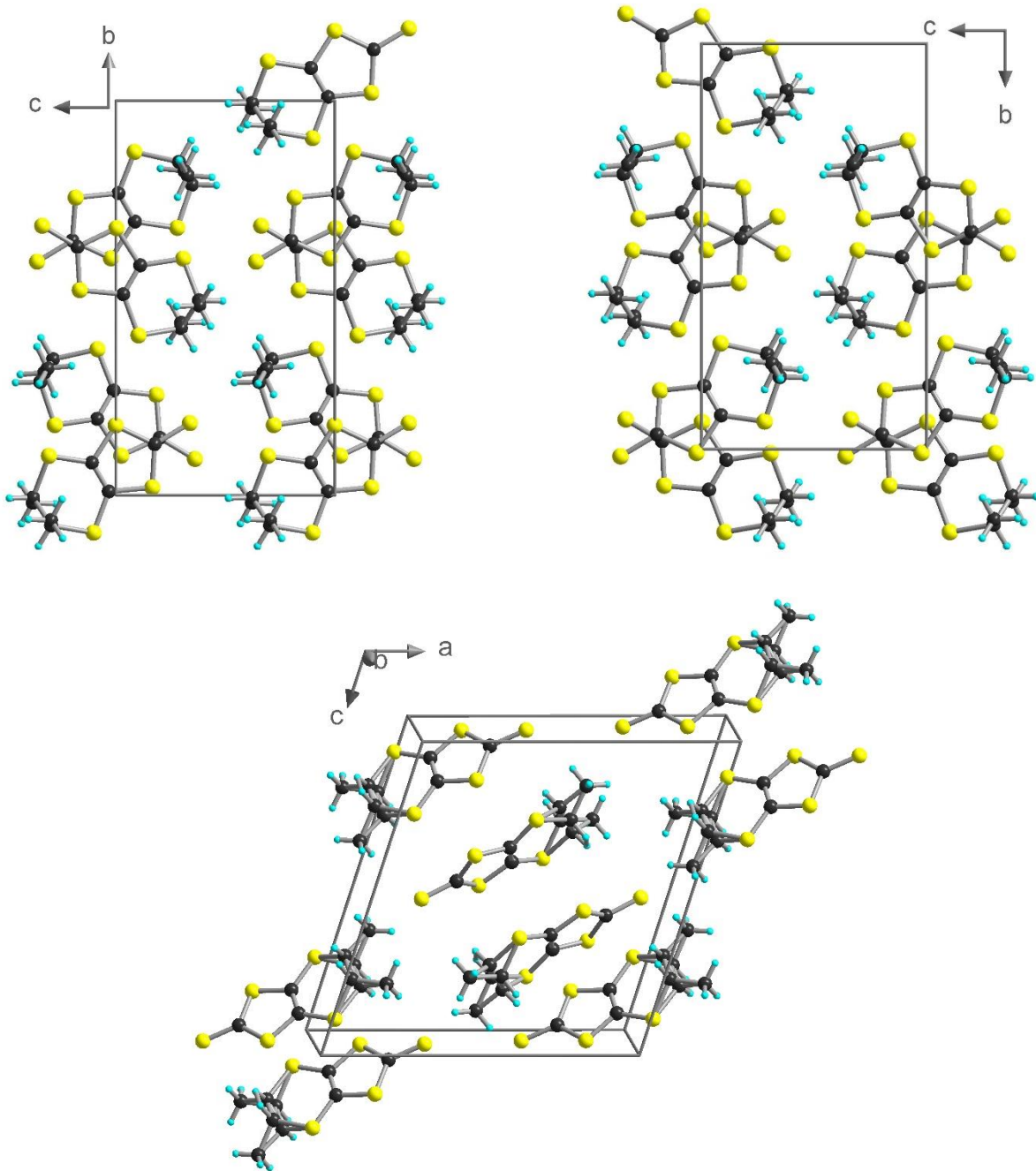
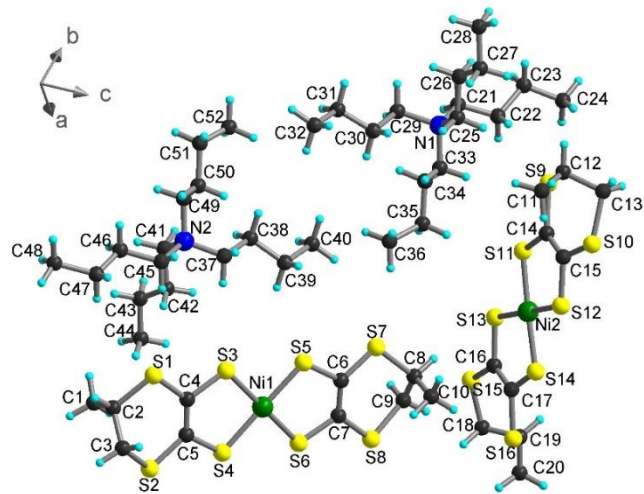


Fig. S49 View of the structures of ***S,S*-dm-dddt-thione** (top left) and ***R,R*-dm-dddt-thione** (top right) in the *bc* plane and ***rac*-dm-dddt-thione** in the *ac* plane (bottom). Color code: C (black), H (cyan), S (yellow).

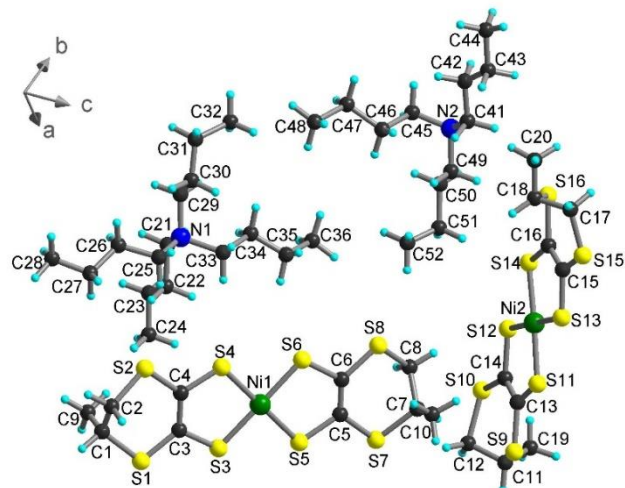
Table S2 Crystallographic data for (TBA)[Ni(S-me-dddt)₂], (TBA)[Ni(R-me-dddt)₂], (TBA)[Ni(S-me-dddt)(R-me-dddt)] and (TBA)[Ni(S-me-dddt)(R-me-dddt)] obtained by scrambling experiment

	(TBA) [Ni(S-me-dddt) ₂]	(TBA) [Ni(R-me-dddt) ₂]	(TBA) [Ni(S-me-dddt) (R-me-dddt)]	(TBA) [Ni(S-me-dddt) (R-me-dddt)] scrambling
Empirical formula	C ₂₆ H ₄₈ NNiS ₈			
Fw	689.84	689.84	689.84	689.84
Crystal color	Green	Green	Green	Green
Crystal size (mm ³)	0.05*0.03*0.02	0.10*0.03*0.02	0.12*0.08*0.02	0.12*0.06*0.03
Temperature (K)	150	150	150	150
Wavelength (Å)	1.54184	1.54154	1.54184	1.54184
Crystal system, Z	Triclinic, 2	Triclinic, 2	Triclinic, 2	Triclinic, 2
Space group	P1	P1	P-1	P-1
a (Å)	9.3775 (4)	9.3629 (7)	9.3679 (7)	9.3463 (5)
b (Å)	13.5118 (4)	13.5340 (7)	13.5115 (10)	13.4804 (8)
c (Å)	13.7352 (5)	13.7348 (7)	13.8074 (9)	13.8283 (7)
α (°)	83.682 (3)	83.774 (4)	83.771 (6)	83.785 (4)
β (°)	77.681 (3)	77.788 (5)	76.905 (6)	76.530 (5)
γ (°)	87.481 (3)	87.427 (5)	87.281 (6)	87.594 (5)
V (Å ³)	1689.57 (11)	1690.59 (18)	1691.7 (2)	1684.12 (16)
ρ _{calc} (g.cm ⁻³)	1.356	1.355	1.354	1.360
μ(CuKα) (mm ⁻¹)	5.571	5.567	5.564	5.589
θ range (°)	3.292–73.696	3.286–74.116	3.291–73.612	3.298–73.189
Data collected	28197	27719	12886	26519
Data unique	12527	12475	6561	6435
Data observed	9826	8028	4648	5140
R(int)	0.0376	0.0566	0.0387	0.0449
Nb of parameters / restraints	649/47	649/78	346/27	346/34
Flack parameter	0.105 (18)	0.12 (3)	-	-
R1(F), ^a I > 2σ(I)	0.0705	0.0744	0.0824	0.1046
wR2(F ²), ^b all data	0.2060	0.2255	0.2421	0.3208
S(F ²), ^c all data	1.063	1.059	1.069	1.136

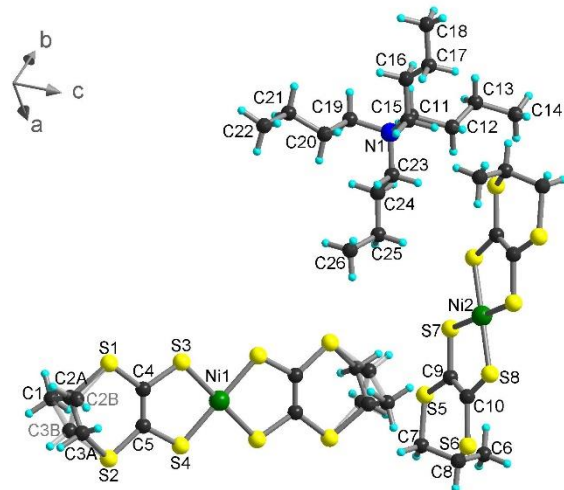
^aR1(F) = Σ||F₀|-|F_c||/Σ|F₀|; ^bwR2(F²) = [Σw(F₀²-F_c²)²/ΣwF₀⁴]^{1/2}; ^cS(F²) = [Σw(F₀²-F_c²)²/(n+r-p)]^{1/2}.



(a)



(b)



(c)

Fig. S50 Structure of $(\text{TBA})[\text{Ni}(\text{S-me-dddt})_2]$ (a), $(\text{TBA})[\text{Ni}(\text{R-me-dddt})_2]$ (b) and $(\text{TBA})[\text{Ni}(\text{S-me-dddt})(\text{R-me-dddt})]$ (c) with atom label.

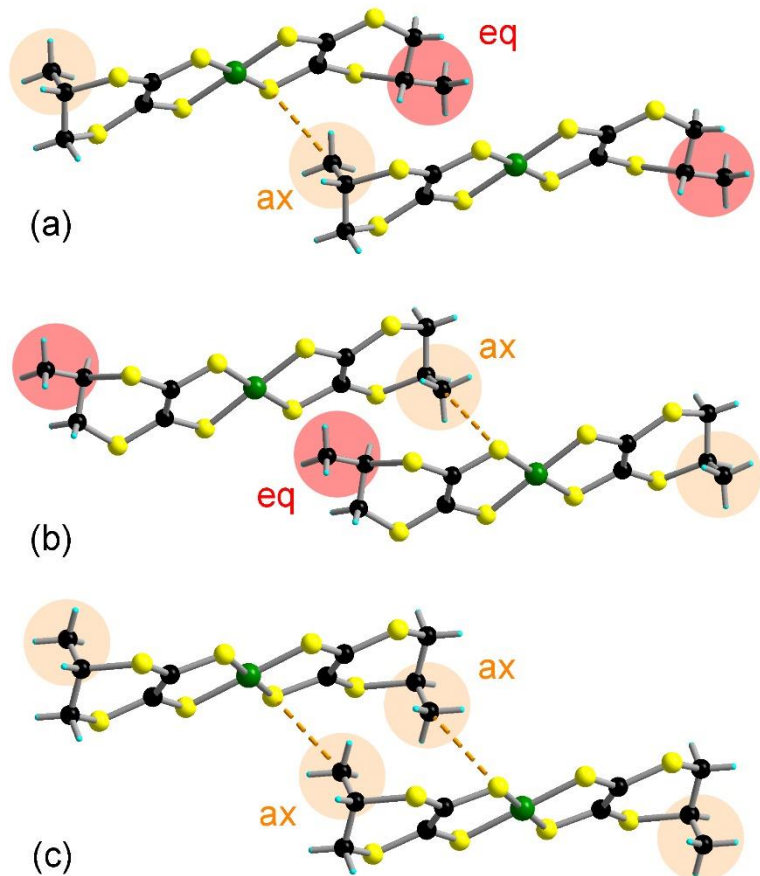


Fig. S51 Highlighting axial and equatorial positions of the methyl substituents from two consecutive *trans* isomers in $(TBA)[Ni(S\text{-}me\text{-}dddt})_2]$ (a), $(TBA)[Ni(R\text{-}me\text{-}dddt})_2]$ (b) and $(TBA)[Ni(S\text{-}me\text{-}dddt})(R\text{-}me\text{-}dddt})]$ (c). The resulting C–H…S intermolecular interactions are represented in orange dashed lines. Color code: C (black), H (cyan), S (yellow), Ni (green).

Table S3 Crystallographic data for (TBA)[Ni(S,S-dm-dddt)(R,R-dm-dddt)]

	(TBA) [Ni(S,S-dm-dddt) (R,R-dm-dddt)]	(TBA) [Ni(S,S-dm-dddt) (R,R-dm-dddt)] scrambling
Empirical formula	C ₂₈ H ₅₂ NNiS ₈	C ₂₈ H ₅₂ NNiS ₈
Fw	717.89	717.89
Crystal color	Green	Green
Crystal size (mm ³)	0.28*0.25*0.08	0.28*0.25*0.08
Temperature (K)	297	297
Wavelength (Å)	1.54184	1.54184
Crystal system, Z	Triclinic, 2	Triclinic, 2
Space group	P-1	P-1
a (Å)	9.9746 (3)	9.9129 (2)
b (Å)	12.8587 (4)	12.6872 (4)
c (Å)	15.4306 (5)	15.3643 (5)
α (°)	81.684 (3)	81.603 (3)
β (°)	80.287 (3)	80.128 (2)
γ (°)	69.560 (3)	68.888 (3)
V (Å ³)	1820.05 (11)	1768.45 (10)
ρ _{calc} (g.cm ⁻³)	1.310	1.348
μ(CuKα) (mm ⁻¹)	5.192	5.343
θ range (°)	2.918–73.509	2.932–76.323
Data collected	12621	29990
Data unique	7089	7142
Data observed	6001	6981
R(int)	0.0334	0.0336
Nb of parameters / restraints	382/2	382/7
Flack parameter	-	-
R1(F), ^a I > 2σ(I)	0.0516	0.0451
wR2(F ²), ^b all data	0.1639	0.1268
S(F ²), ^c all data	1.055	0.995

^aR1(F) = Σ||F₀|-|F_c||/Σ|F₀|; ^bwR2(F²) = [Σw(F₀²-F_c²)²/ΣwF₀⁴]^{1/2}; ^cS(F²) = [Σw(F₀²-F_c²)²/(n+r-p)]^{1/2}.

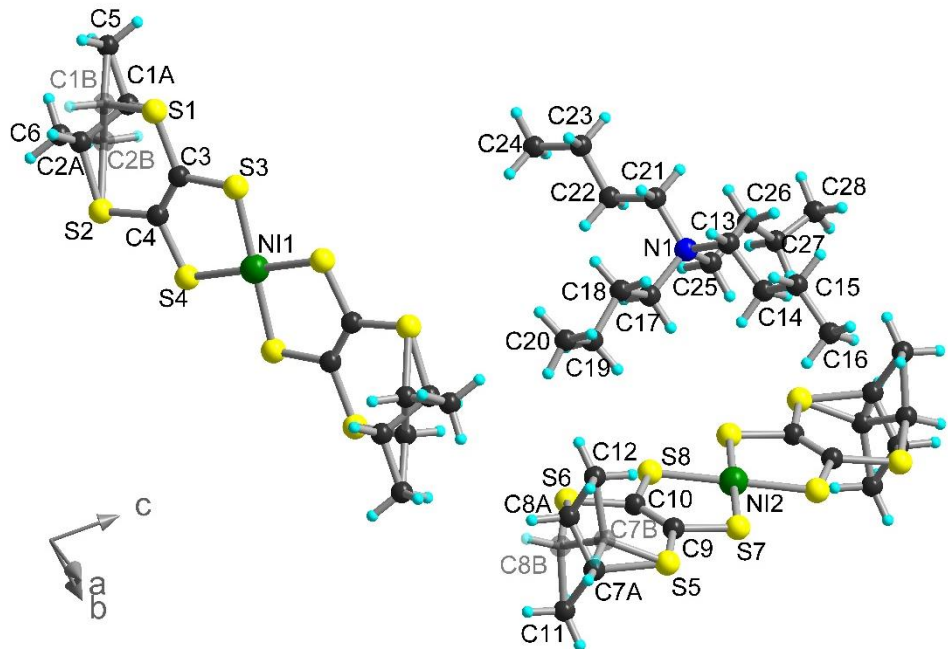
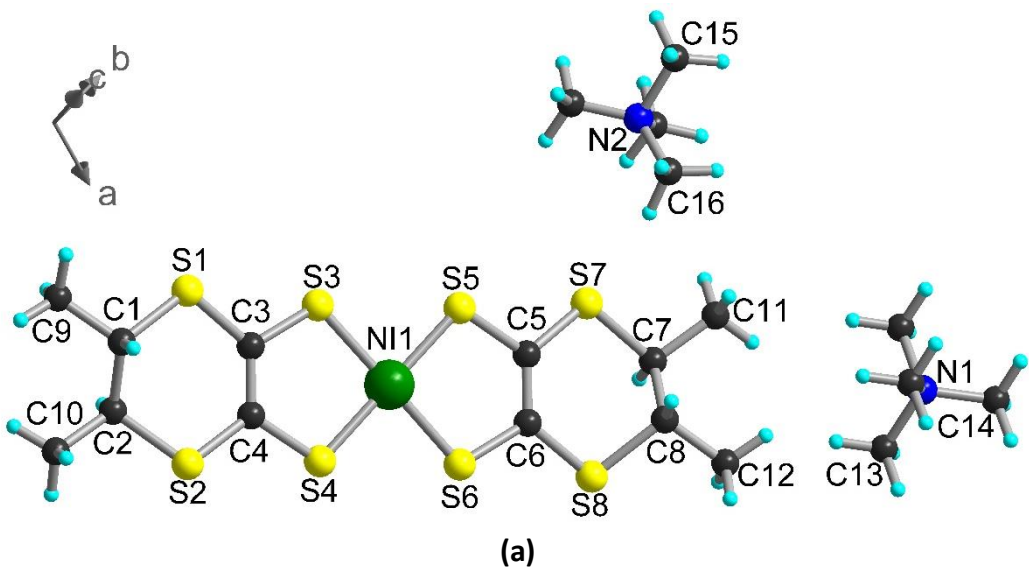


Fig. S52 View of the structure of (TBA)[Ni(*S,S*-dm-dddt)(*R,R*-dm-dddt)].

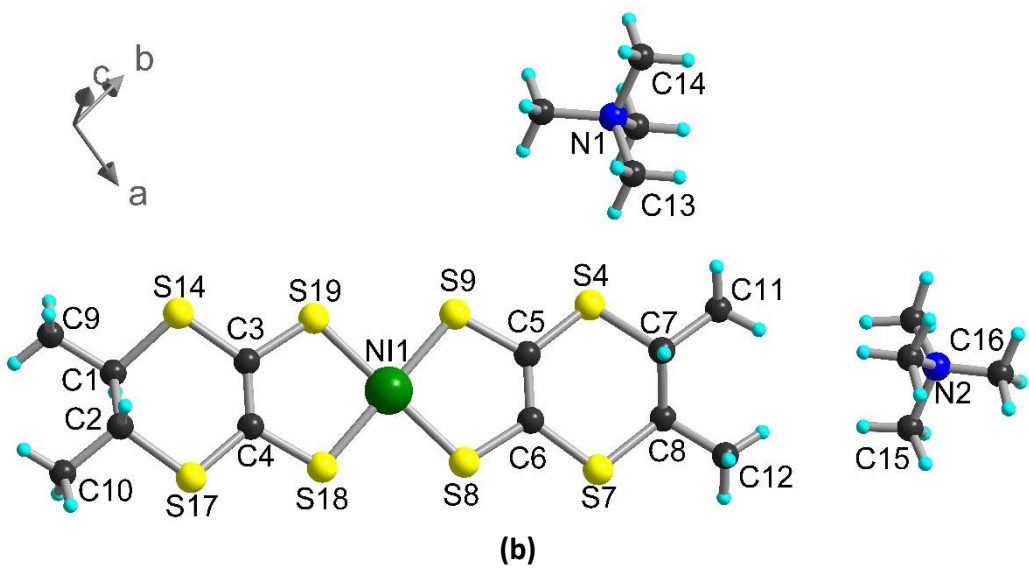
Table S4 Crystallographic data for (TMA)[Ni(S,S-dm-dddt)₂], (TMA)[Ni(R,R-dm-dddt)₂] and (TMA)[Ni(S,S-dm-dddt)(R,R-dm-dddt)]

	(TMA) [Ni(S,S-dm-dddt) ₂]	(TMA) [Ni(R,R-dm-dddt) ₂]	(TMA) [Ni(S,S-dm-dddt) (R,R-dm-dddt)]
Empirical formula	C ₁₆ H ₂₈ NNiS ₈	C ₁₆ H ₂₈ NNiS ₈	C ₁₆ H ₂₈ NNiS ₈
Fw	549.58	549.58	549.58
Crystal color	Green	Green	Green
Crystal size (mm ³)	0.2*0.17*0.09	0.28*0.25*0.12	0.15*0.11*0.05
Temperature (K)	150	150	150
Wavelength (Å)	1.54184	1.54184	1.54184
Crystal system, Z	Monoclinic, 4	Monoclinic, 4	Monoclinic, 4
Space group	I2	I2	I2/a
a (Å)	17.5736 (4)	17.5730 (5)	27.1336 (11)
b (Å)	9.9714 (2)	9.9665 (2)	9.9785 (3)
c (Å)	15.7038 (4)	15.7025 (5)	15.7836 (7)
α (°)	90	90	90
β (°)	119.990 (3)	119.996 (4)	145.935 (3)
γ (°)	90	90	90
V (Å ³)	2383.39 (11)	2381.80 (14)	2393.70 (19)
ρ _{calc} (g.cm ⁻³)	1.532	1.533	1.525
μ(CuKα) (mm ⁻¹)	7.745	7.750	7.712
θ range (°)	3.091–72.063	3.091–71.946	5.303–73.476
Data collected	10593	10384	4853
Data unique	4505	4411	2329
Data observed	4450	4371	2084
R(int)	0.0186	0.0188	0.0266
Nb of parameters / restraints	226/14	231/1	138/0
Flack parameter	0.022 (10)	0.038 (10)	-
R1(F), ^a I > 2σ(I)	0.0301	0.0295	0.0387
wR2(F ²), ^b all data	0.0856	0.0846	0.1147
S(F ²), ^c all data	1.076	1.055	1.106

^aR1(F) = Σ||F₀|-|F_c||/Σ|F₀|; ^bwR2(F²) = [Σw(F₀²-F_c²)²/ΣwF₀⁴]^{1/2}; ^cS(F²) = [Σw(F₀²-F_c²)²/(n+r-p)]^{1/2}.



(a)



(b)

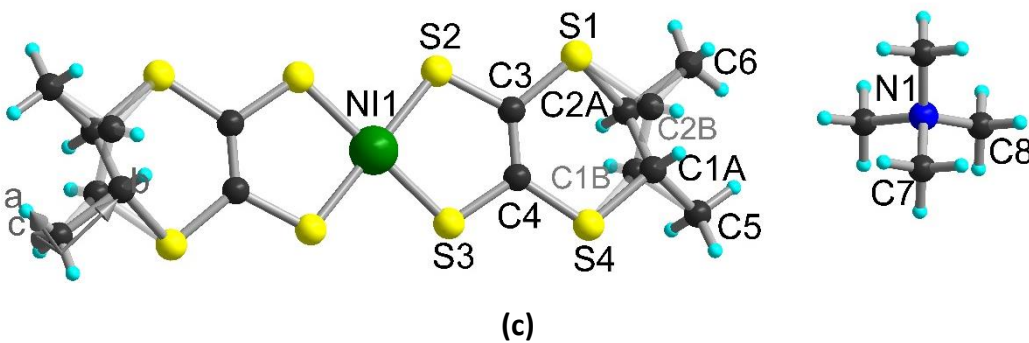


Fig. S53 Structures of $(\text{TMA})[\text{Ni}(\text{S},\text{S}-\text{dm-dddt})_2]$ (a), $(\text{TMA})[\text{Ni}(\text{R},\text{R}-\text{dm-dddt})_2]$ (b) and $(\text{TMA})[\text{Ni}(\text{S},\text{S}-\text{dm-dddt})(\text{R},\text{R}-\text{dm-dddt})]$ (c) with atom label.

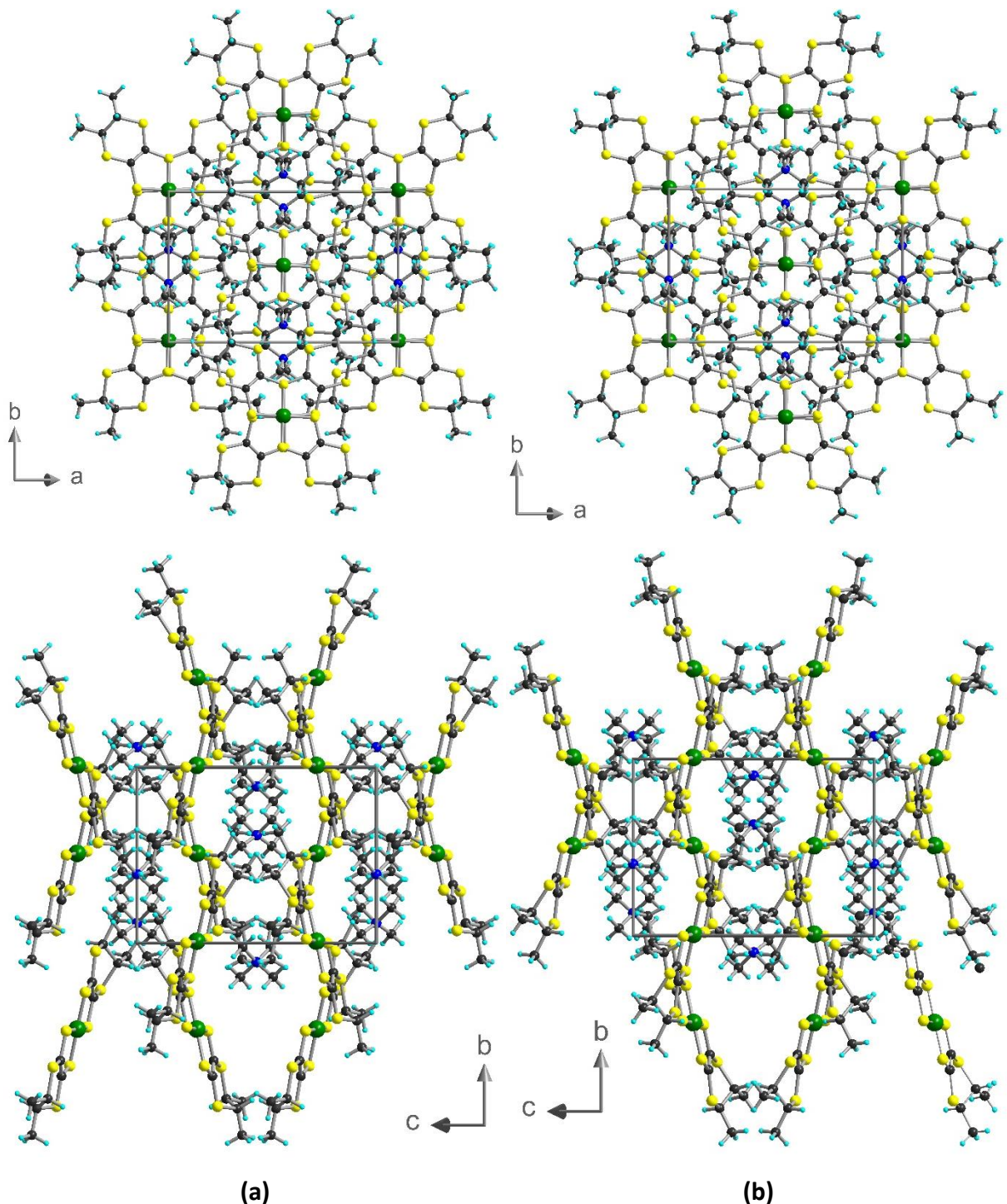


Fig. S54 Structures of $(\text{TMA})[\text{Ni}(\text{S},\text{S}-\text{dm-dddt})_2]$ (a) and $(\text{TMA})[\text{Ni}(\text{R},\text{R}-\text{dm-dddt})_2]$ (b) in the ab plane (top) and bc plane (bottom). Color code: C (black), H (cyan), N (blue), S (yellow), Ni (green).

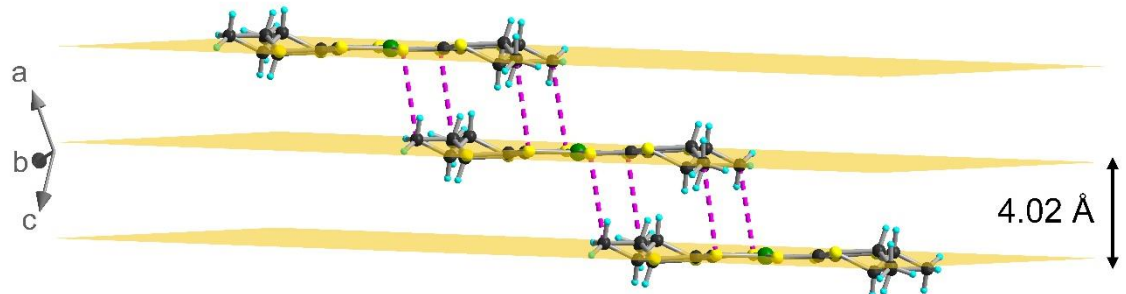


Fig. S55 Distance between planes of complexes in **(TMA)[Ni(S,S-dm-dddt)(R,R-dm-dddt)]**. Color code: C (black), H (cyan), S (yellow), Ni (green).

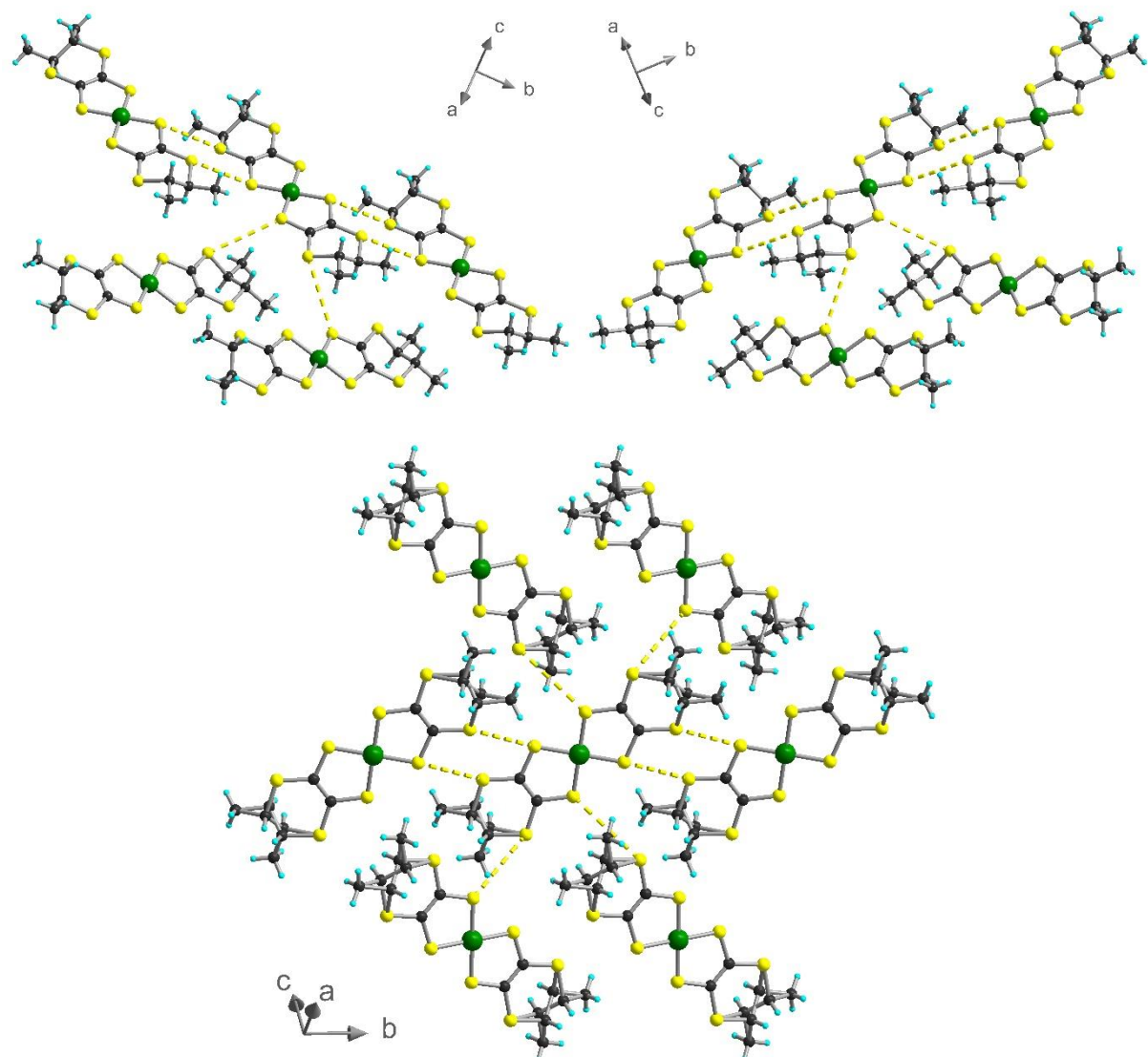
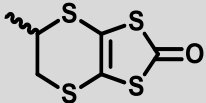


Fig. S56 Intermolecular S···S interactions below 4.50 Å between neighbouring complexes in **(TMA)[Ni(S,S-dm-dddt)₂]**, **(TMA)[Ni(R,R-dm-dddt)₂]** (top) and **(TMA)[Ni(S,S-dm-dddt)(R,R-dm-dddt)]** (bottom).

Table S5 Crystallographic data for $[\text{Ni}(S\text{-me-dddt})_2]$, $[\text{Ni}(R\text{-me-dddt})_2]$ and $[\text{Ni}(S\text{-me-dddt})(R\text{-me-dddt})]$

	$[\text{Ni}(S\text{-me-dddt})_2]$	$[\text{Ni}(R\text{-me-dddt})_2]$	$[\text{Ni}(S\text{-me-dddt})(R\text{-me-dddt})]$
Empirical formula	$\text{C}_{10}\text{H}_{12}\text{NiS}_8$	$\text{C}_{10}\text{H}_{12}\text{NiS}_8$	$\text{C}_{10}\text{H}_{12}\text{NiS}_8$
Fw	447.39	447.39	447.39
Crystal color	Black	Black	Black
Crystal size (mm ³)	0.12*0.04*0.02	0.27*0.06*0.03	0.28*0.08*0.04
Temperature (K)	150	150	150
Wavelength (Å)	1.54184	1.54184	1.54184
Crystal system, Z	Monoclinic, 2	Monoclinic, 2	Monoclinic, 2
Space group	$P2_1$	$P2_1$	$P2_1/c$
a (Å)	5.2529 (2)	5.2567 (6)	5.2521 (2)
b (Å)	15.0859 (4)	15.0900 (19)	15.1161 (5)
c (Å)	10.1409 (3)	10.1421 (12)	10.1483 (3)
α (°)	90	90	90
β (°)	90.135 (3)	90.093 (11)	90.181 (4)
γ (°)	90	90	90
V (Å ³)	803.61 (4)	804.51 (17)	805.68 (5)
ρ_{calc} (g.cm ⁻³)	1.849	1.847	1.844
$\mu(\text{CuK}\alpha)$ (mm ⁻¹)	11.306	11.293	11.277
θ range (°)	4.360–73.517	4.359–74.843	5.250–73.106
Data collected	7587	5115	4209
Data unique	2969	3010	1476
Data observed	2777	2679	1426
R(int)	0.0292	0.0486	0.0531
Nb of parameters / restraints	172/1	172/1	88/0
Flack parameter	0.05 (3)	0.15 (6)	-
$R1(F)$, ^a $ I > 2\sigma(I)$	0.0363	0.0647	0.0631
$wR2(F^2)$, ^b all data	0.0963	0.1802	0.1709
$S(F^2)$, ^c all data	1.127	1.076	1.144

^a $R1(F) = \sum |F_0| - |F_c| / \sum |F_0|$; ^b $wR2(F^2) = [\sum w(F_0^2 - F_c^2)^2 / \sum wF_0^4]^{1/2}$; ^c $S(F^2) = [\sum w(F_0^2 - F_c^2)^2 / (n+r-p)]^{1/2}$.

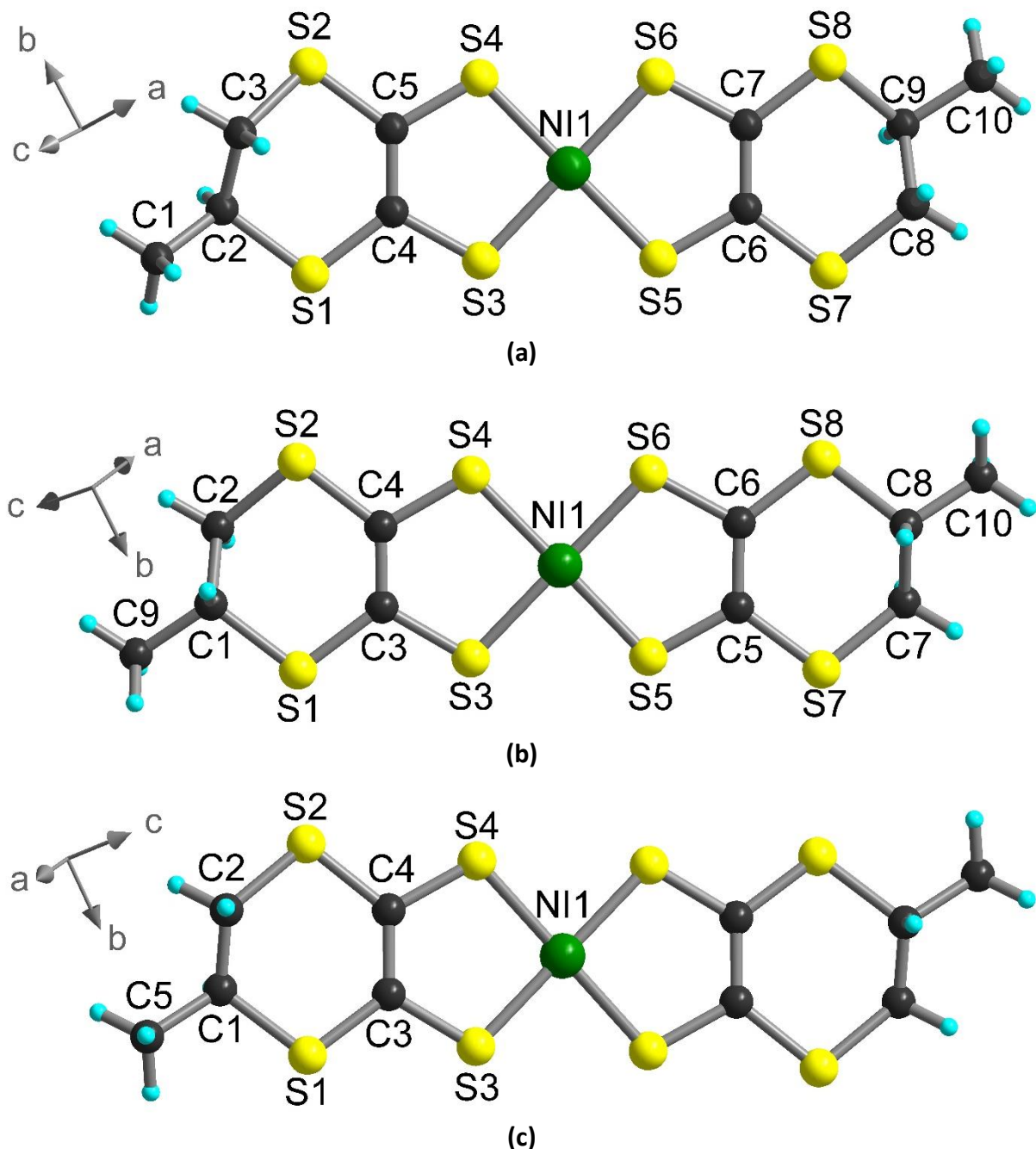


Fig. S57 Structures of $[\text{Ni}(\text{S-me-dddt})_2]$ (a), $[\text{Ni}(\text{R-me-dddt})_2]$ (b) and $[\text{Ni}(\text{S-me-dddt})(\text{R-me-dddt})]$ (c) with atom label.

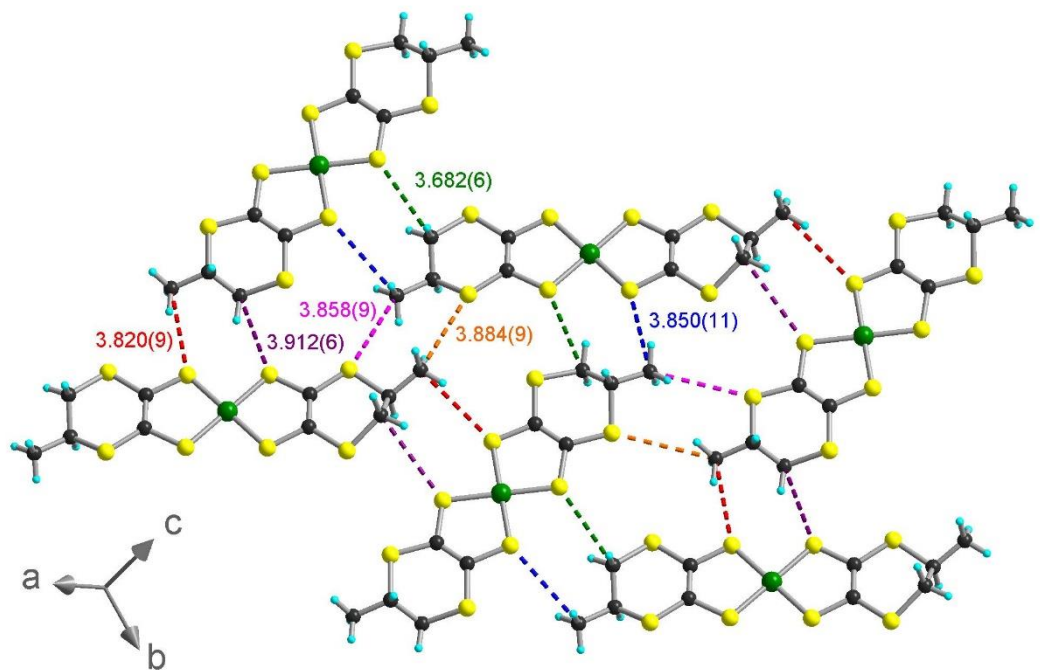


Fig. S58 “In plane” intermolecular C-H…S interactions between neighbouring complexes in **[Ni(S-mddt)₂]**. Color code: C (black), H (cyan), S (yellow), Ni (green). Different colours are used to discriminate each interaction.

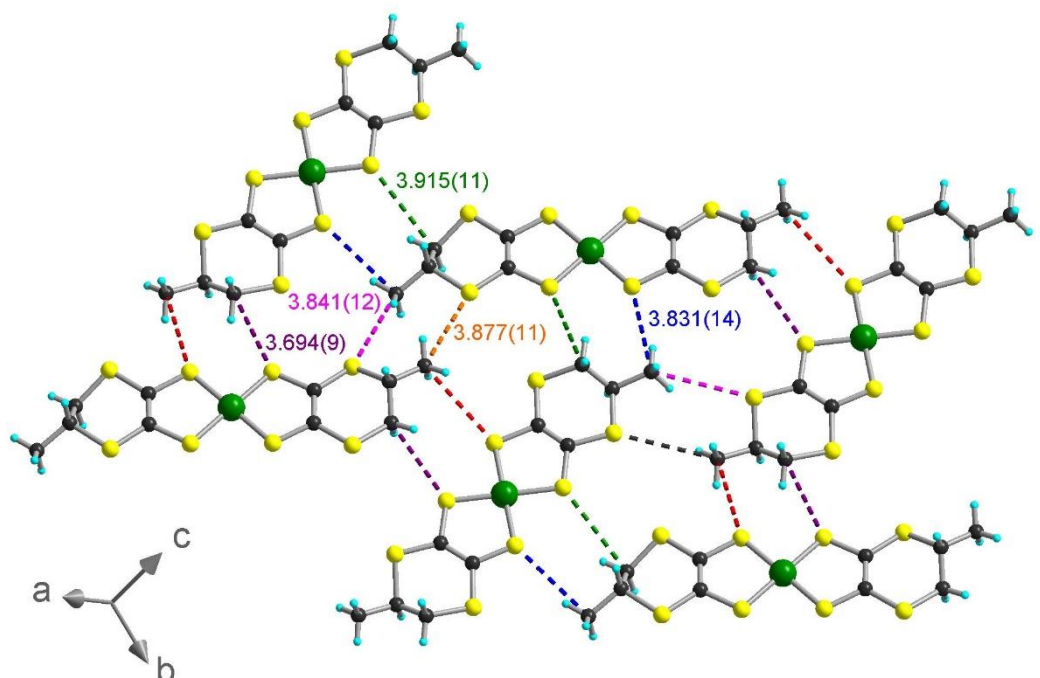


Fig. S59 “In plane” intermolecular C-H…S interactions between neighbouring complexes in **[Ni(R-mddt)₂]**. Color code: C (black), H (cyan), S (yellow), Ni (green). Different colours are used to discriminate each interaction.

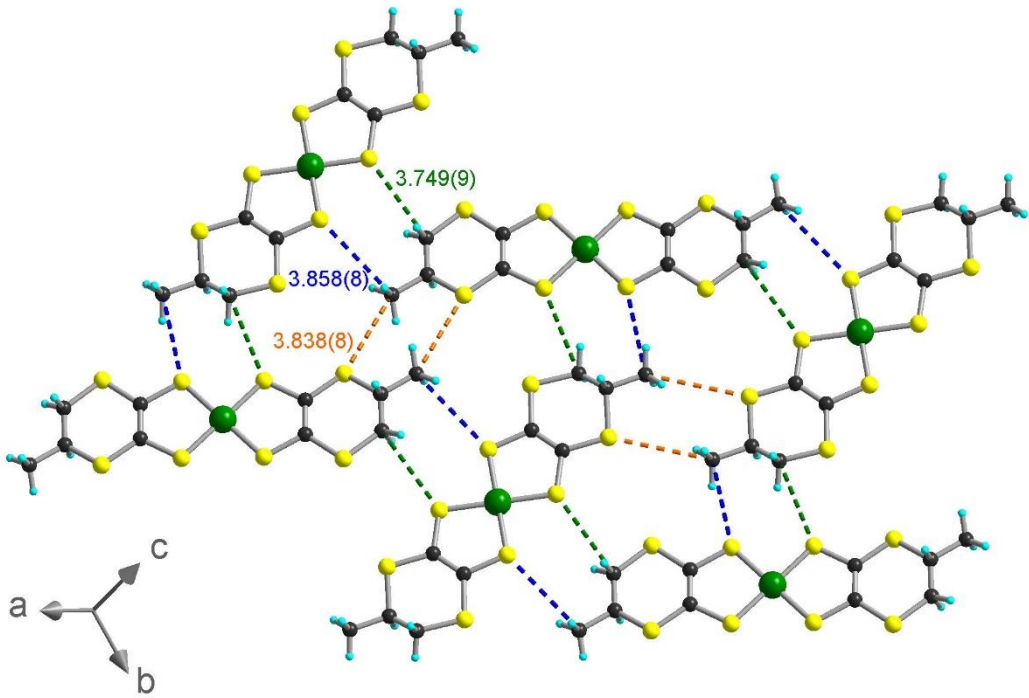


Fig. S60 “In plane” intermolecular C-H···S interactions between neighbouring complexes in **[Ni(S-me-dddt)(R-me-dddt)]**. Color code: C (black), H (cyan), S (yellow), Ni (green). Different colours are used to discriminate each interaction.

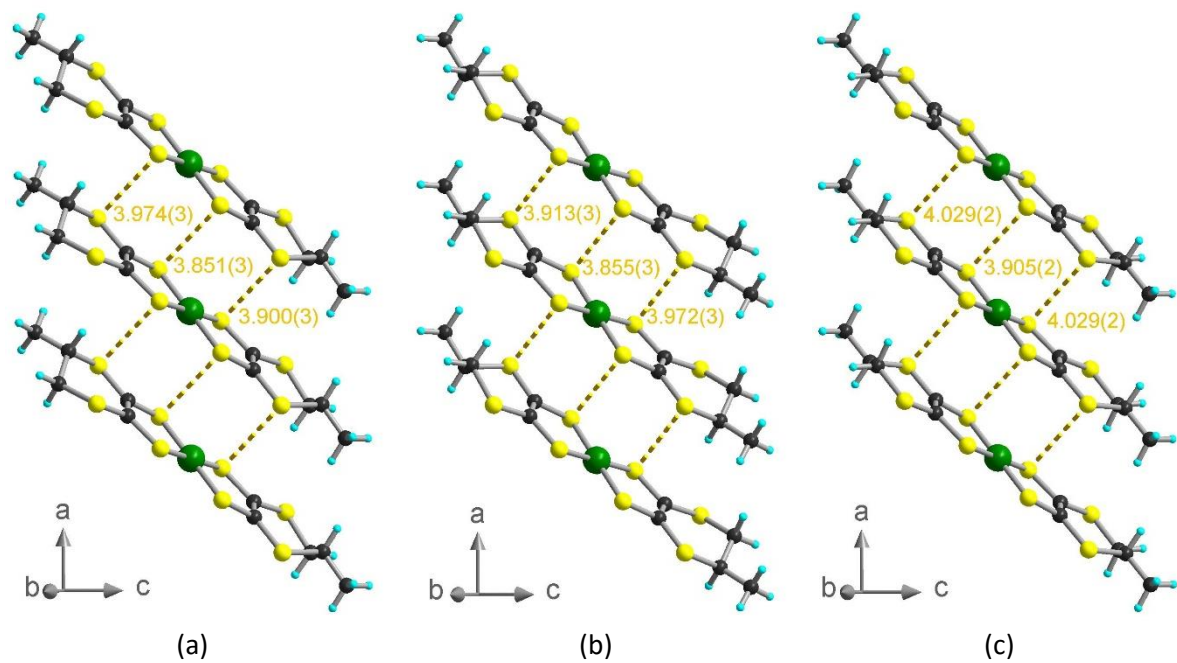
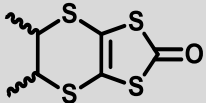


Fig. S61 “Out-of-plane” intermolecular S···S interactions between neighbouring complexes in (a) **[Ni(S-me-dddt)₂]**, (b) **[Ni(R-me-dddt)₂]** and (c) **[Ni(S-me-dddt)(R-me-dddt)]**. Color code: C (black), H (cyan), S (yellow), Ni (green).

Table S6 Crystallographic data for $[\text{Ni}(S,S\text{-dm-dddt})_2]$, $[\text{Ni}(R,R\text{-dm-dddt})_2]$ and $[\text{Ni}(S,S\text{-dm-dddt})(R,R\text{-dm-dddt})]$

	$[\text{Ni}(S,S\text{-dm-dddt})_2]$	$[\text{Ni}(R,R\text{-dm-dddt})_2]$	$[\text{Ni}(S,S\text{-dm-dddt})(R,R\text{-dm-dddt})]$
Empirical formula	$\text{C}_{12}\text{H}_{16}\text{NiS}_8$	$\text{C}_{12}\text{H}_{16}\text{NiS}_8$	$\text{C}_{12}\text{H}_{16}\text{NiS}_8$
Mw	475.44	475.44	475.44
Crystal color	Black	Black	Black
Crystal size (mm ³)	0.12*0.04*0.02	0.20*0.15*0.13	0.20*0.20*0.16
Temperature (K)	150	293	150
Wavelength (Å)	1.54184	0.71073	1.54184
Crystal system, Z	Triclinic, 1	Triclinic, 1	Triclinic, 1
Space group	<i>P</i> 1	<i>P</i> 1	<i>P</i> -1
a (Å)	6.9052 (3)	6.9784 (4)	6.9552 (7)
b (Å)	7.7527 (3)	7.8994 (6)	7.8717 (8)
c (Å)	9.1468 (3)	9.2170 (5)	9.1681 (9)
α (°)	70.732 (4)	70.105 (6)	69.989 (9)
β (°)	76.045 (3)	75.451 (5)	74.837 (8)
γ (°)	76.463 (4)	75.277 (4)	72.895 (9)
V (Å ³)	442.17 (3)	454.44 (5)	443.49 (8)
ρ_{calc} (g.cm ⁻³)	1.785	1.737	1.780
μ (mm ⁻¹)	10.315 (CuK α)	1.975 (MoK α)	10.284 (CuK α)
θ range (°)	5.206–72.040	3.63–29.99	5.22–73.76
Data collected	5909	10223	2933
Data unique	3083	4578	1716
Data observed	3010	3728	1644
R(int)	0.0174	0.0241	0.0199
Nb of parameters / restraints	190/3	190/3	115/0
Flack parameter	0.038 (11)	0.017 (12)	-
$R1(F)$, ^a $ F > 2\sigma(F)$	0.0212	0.0267	0.0371
$wR2(F^2)$, ^b all data	0.0575	0.0610	0.1108
$S(F^2)$, ^c all data	1.049	1.019	1.141

^a $R1(F) = \sum |F_0| - |F_c| / \sum |F_0|$; ^b $wR2(F^2) = [\sum w(F_0^2 - F_c^2)^2 / \sum wF_0^4]^{1/2}$; ^c $S(F^2) = [\sum w(F_0^2 - F_c^2)^2 / (n+r-p)]^{1/2}$.

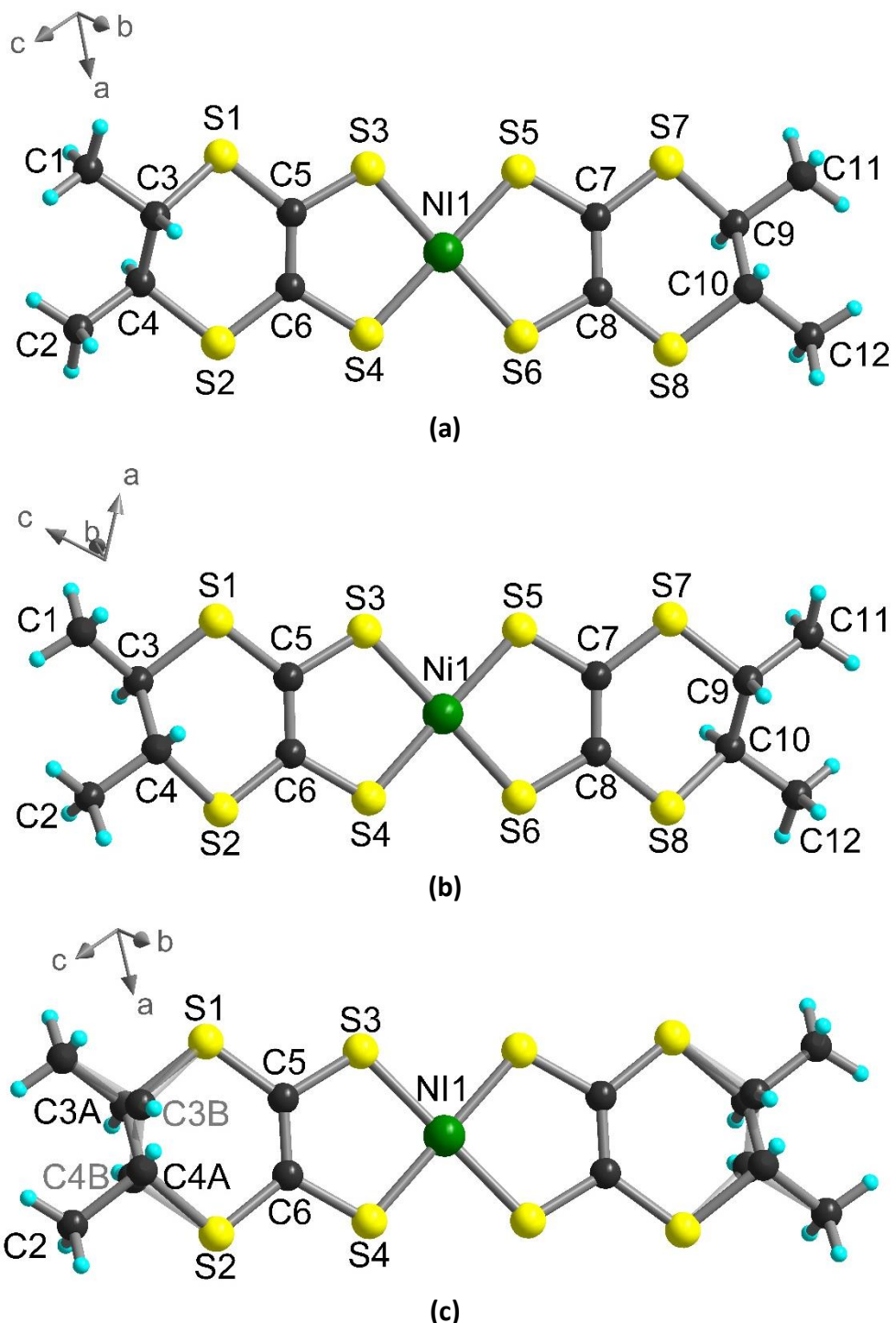
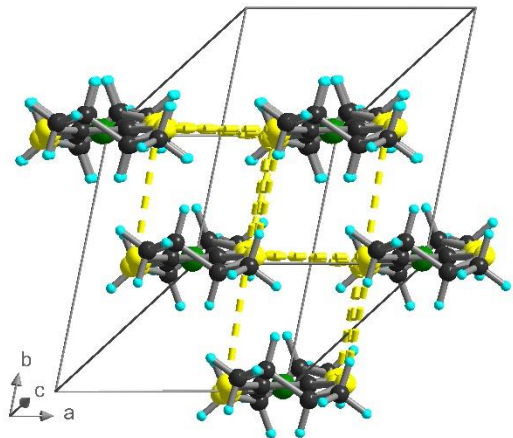
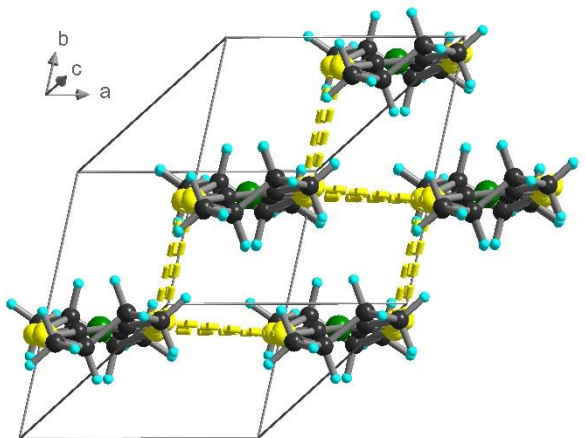


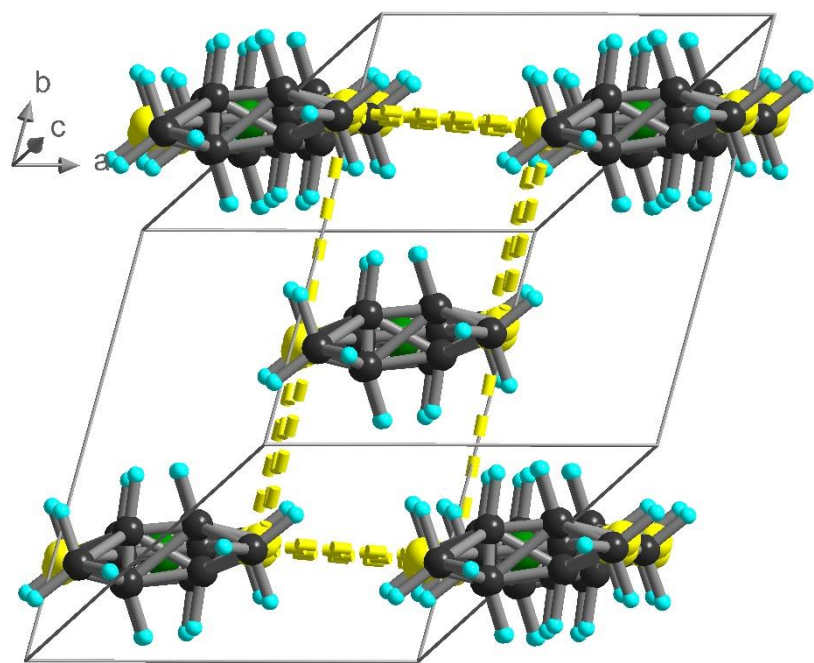
Fig. S62 Structures of $[\text{Ni}(\text{S},\text{S}-\text{dm-dddt})_2]$ (a), $[\text{Ni}(\text{R},\text{R}-\text{dm-dddt})_2]$ (b) and $[\text{Ni}(\text{S},\text{S}-\text{dm-dddt})(\text{R},\text{R}-\text{dm-dddt})]$ (c) with atom label.



(a)



(b)



(c)

Fig. S63 View of the crystal packing in $[\text{Ni}(S,S\text{-dm-dddt})_2]$ (a), $[\text{Ni}(R,R\text{-dm-dddt})_2]$ (b) and $[\text{Ni}(S,S\text{-dm-dddt})(R,R\text{-dm-dddt})]$ (c).

Band structure calculations

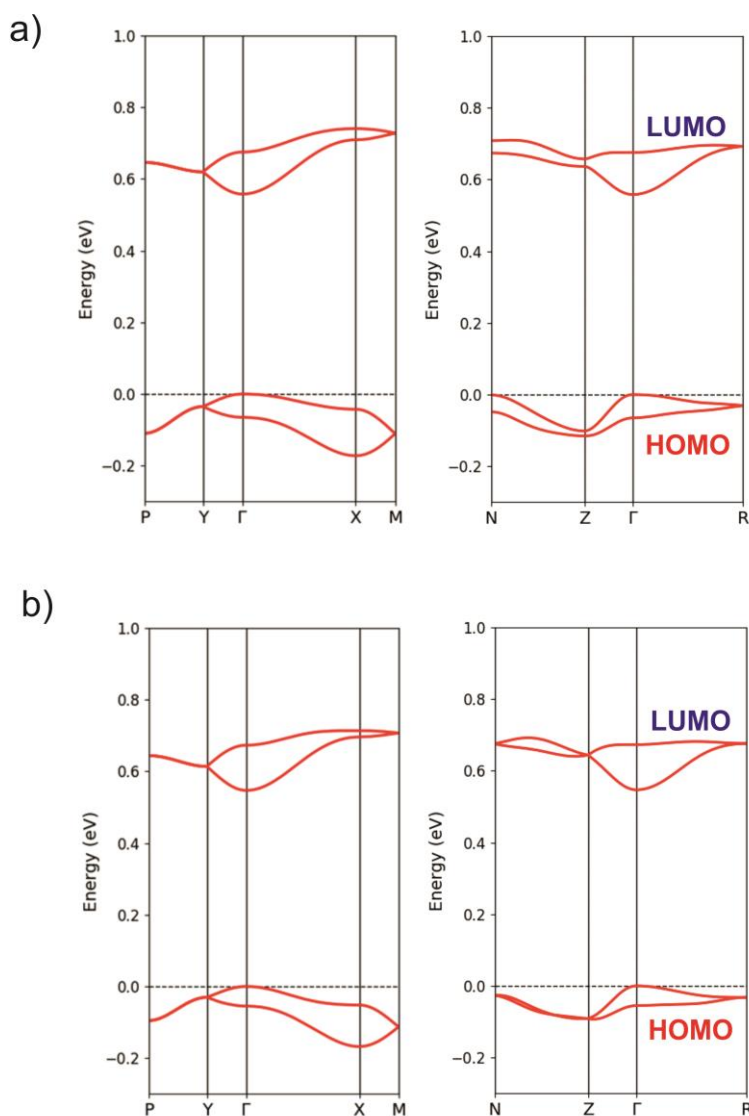


Fig. S64 DFT band structure for the neutral solids $[\text{Ni}(\text{S-me-dddt})_2]$ (a) and $[\text{Ni}(\text{S-me-dddt})(\text{R-me-dddt})]$ (b). $\Gamma=(0, 0, 0)$, $X=(a^*/2, 0, 0)$, $Y=(0, b^*/2, 0)$, $Z=(0, 0, c^*/2)$, $M=(a^*/2, b^*/2, 0)$, $P=(0, b^*/2, c^*/2)$, $N=(a^*/2, 0, c^*/2)$ and $R=(a^*/2, b^*/2, c^*/2)$. The dashed line refers to the highest occupied level.

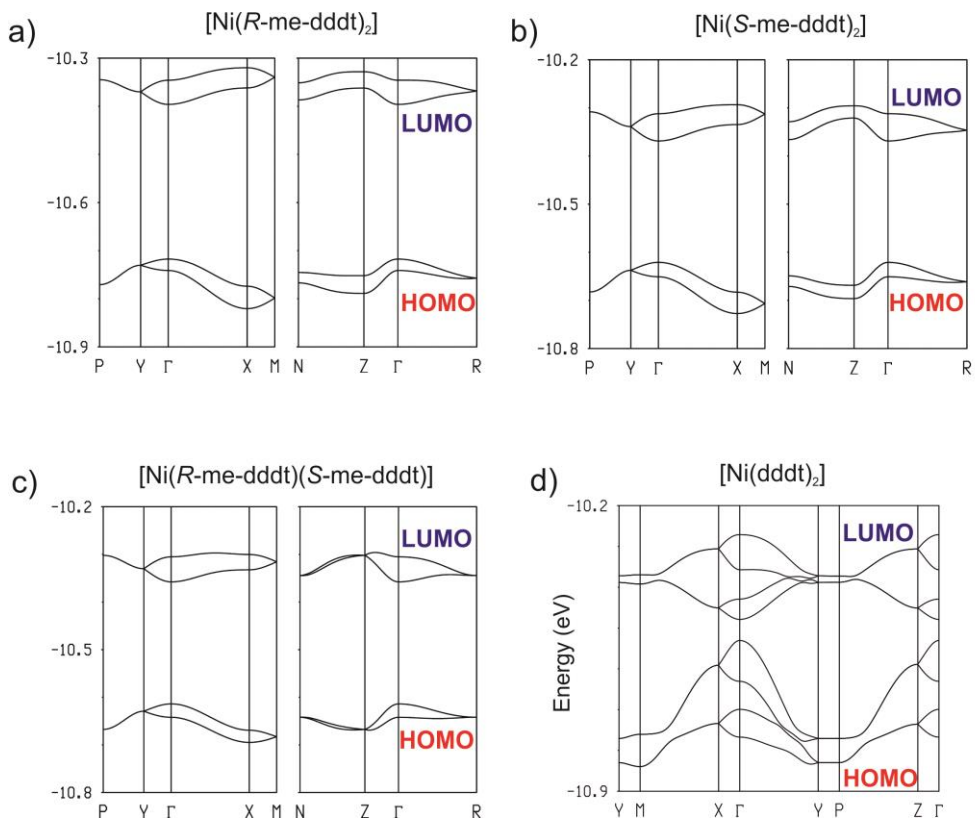


Fig. S65 Extended Hückel band structure for the neutral solids $[\text{Ni}(R\text{-me-dddt})_2]$ (a) $[\text{Ni}(S\text{-me-dddt})_2]$ (b) and $[\text{Ni}(S\text{-me-dddt})(R\text{-me-dddt})]$ (c) as well as for the parent system $[\text{Ni}(\text{dddt})_2]$ (d). $\Gamma = (0, 0, 0)$, $X = (\sigma^*/2, 0, 0)$, $Y = (0, b^*/2, 0)$, $Z = (0, 0, c^*/2)$, $M = (\sigma^*/2, b^*/2, 0)$, $P = (0, b^*/2, c^*/2)$, $R = (\sigma^*/2, b^*/2, c^*/2)$ and $N = (\sigma^*/2, 0, c^*/2)$. The dashed line refers to the highest occupied level.

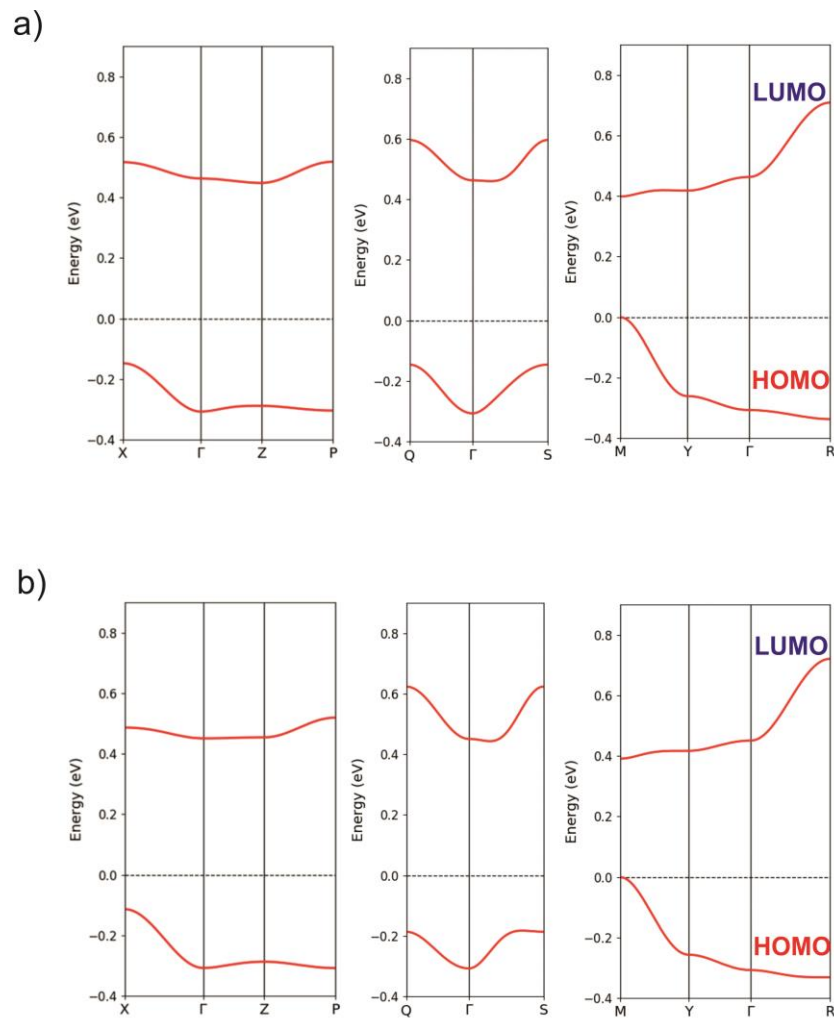


Fig. S66 DFT band structure for the neutral solids $[\text{Ni}(\text{S},\text{S-dm-dddt})_2]$ (a) and $[\text{Ni}(\text{S},\text{S-dm-dddt})(\text{R},\text{R-dm-dddt})]$. $\Gamma = (0, 0, 0)$, $\text{X} = (\alpha^*/2, 0, 0)$, $\text{Y} = (0, b^*/2, 0)$, $\text{Z} = (0, 0, c^*/2)$, $\text{M} = (\alpha^*/2, b^*/2, 0)$, $\text{P} = (0, b^*/2, c^*/2)$, $\text{Q} = (\alpha^*/2, 0, c^*/2)$, $\text{R} = (\alpha^*/2, b^*/2, c^*/2)$ and $\text{S} = (-\alpha^*/2, 0, c^*/2)$. The dashed line refers to the highest occupied level.

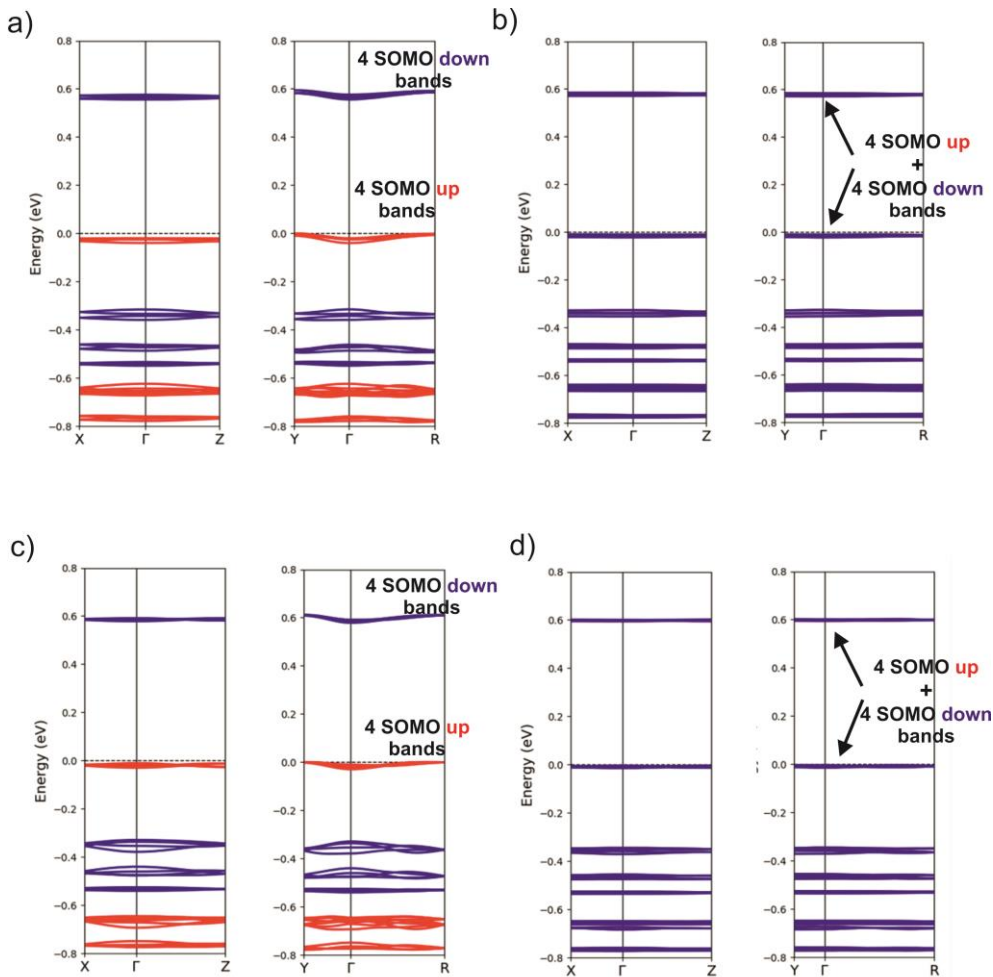


Fig. S67 DFT band structure for the ferromagnetic (FM) (a, c) and antiferromagnetic (AF) (b, d) states of $(\text{TMA})[\text{Ni}(R,R-\text{dm-dddt})_2]$ and $(\text{TMA})[\text{Ni}(S,S-\text{dm-dddt})(R,R-\text{dm-dddt})]$, respectively. Spin up and spin down bands are shown in red and blue, respectively. The FM state is calculated using the crystallographic cell (a, b, c) containing 4 complexes and $\Gamma = (0, 0, 0)$, $Y = (0, b^*/2, 0)$, $Z = (0, 0, c^*/2)$, $R = (a^*/2, b^*/2, c^*/2)$ and $X = (a^*/2, 0, 0)$. The AFM state is calculated using a double cell ($a' = a$, $b' = 2b$ and $c' = c$) containing 8 complexes and $\Gamma = (0, 0, 0)$, $Y = (0, b'^*/2, 0)$, $Z = (0, 0, c'^*/2)$, $R = (a'^*/2, b'^*/2, c'^*/2)$ and $X = (a'^*/2, 0, 0)$. The dashed line refers to the highest occupied level. In (b and d) the spin up and spin down bands are identical although located in spatially different but equivalent sites so that only the blue bands are visible.